multiPlas

multiPlas – elastoplastic material models for Ansys

GENERAL MULTISURFACE PLASTICITY

USER'S MANUAL

September 2021

Release 5.8.0

Ansys / DYNARDO

Dynamic Software and Engineering GmbH

Weimar, Steubenstraße 25, Germany

Guarantee reference

Dynardo GmbH takes greatest care in developing software and tests all products thoroughly. Despite, the user is fully responsible for the application of this software and is obliged to check correctness of the results obtained. Dynardo GmbH takes no liability for any damage caused by the use of this software, by incorrectness of results, or by misinterpretation.

Content

List of figures

List of tables

1. Introduction

This manual describes the use of the material library multiPlas for Ansys.

The elasto-plastic material models in multiPlas enable the user to simulate elasto-plastic effects of artificial materials, e.g. steel or concrete, and natural born materials, e.g. soil or rock, in geotechnics, civil engineering - as well as - mechanical engineering. In the context of finite element calculations with Ansys, multiPlas provides an efficient and robust algorithm for handling single and multi-surface plasticity. The material models are based on elasto-plastic flow functions with associated and non-associated flow rules. One special feature of the multiPlas material models is the combination of isotropic and anisotropic yield conditions.

The multiPlas library provides models for many different materials based on plasticity theory. Typical materials described by these models can be found in geotechnical engineering (rock, jointed rock, sand, soil), civil engineering (concrete, masonry, wood) and mechanical engineering (cast-iron, laminated sheet packages, additive manufacturing). Some of the multiPlas models are directly integrated in Ansys:

- Geomechanical Toolbox:
  - Jointed rock: **TB**, JROCK
  - Mohr-Coulomb: **TB**, MC
  - Concrete: **TB**, CONCRETE
  - Cam-Clay: **TB**, SOIL
- Crushable foam: **TB**, CFOAM

These models are documented in the “Material Reference” of the Ansys “Mechanical APDL” documentation and will not be presented in this manual. The focus of the manual is on the multiPlas models not directly available and not documented in Ansys:

- Sand model for casting simulations
- Cast iron model with implicit creep
- Masonry model
- Wood model
- Orthotropic boxed value model for additive manufacturing
- Cable model
- Laminated sheet package

In Ansys these models can be accessed by the so-called multiPlas-backdoor: **TB**, MULP.

The multiPlas material models are available for structural volume elements, e.g. SOLID 185 or SOLID 186, structural shell elements, e.g. SHELL 181 or SHELL 281, and structural plane elements assuming plane stress, plane strain or axisymmetric conditions, e.g. PLANE 182 or PLANE 183.

1.1. Theory

1.1.1. Basics of elasto-plastic material models in multiPlas

The material models in multiPlas are based on the concept of rate-independent plasticity. This concept is briefly outlined. A detailed description can be found in one of the classical text-books, e.g. Simo and Hughes [10].

Such material models are characterized by an irreversible strain that develops if a certain criterion, defining the elastic domain, is violated. It is assumed that the total strain vector $\boldsymbol{\varepsilon}^{\mathbf{tot}}$ can be split into an elastic part $\boldsymbol{\varepsilon}^{\mathbf{el}}$ and a plastic part $\boldsymbol{\varepsilon}^{\mathbf{pl}}$

$$\boldsymbol{\varepsilon}^{tot} = \boldsymbol{\varepsilon}^{el} + \boldsymbol{\varepsilon}^{pl} \tag{1.1}$$

The stresses $\boldsymbol{\sigma}$ are related to the elastic strains by the linear elastic material matrix $\mathbf{C}$

$$\boldsymbol{\sigma} = \mathbf{C}\,\boldsymbol{\varepsilon}^{el} = \boldsymbol{C}\left[\boldsymbol{\varepsilon}^{tot} - \boldsymbol{\varepsilon}^{pl}\right] \tag{1.2}$$

Furthermore, it is assumed that the plastic strains develop instantaneously, i. e., independent of time.

In the stress space the elastic domain is defined by the yield function F

$$F(\boldsymbol{\sigma}, \boldsymbol{\kappa}) \leq 0 \tag{1.3}$$

where $\boldsymbol{\kappa}$is the vector of hardening/softening variables. An elastic state is represented by

$$F(\boldsymbol{\sigma}, \boldsymbol{\kappa}) < 0 \tag{1.4}$$

The yield surface

$$F(\boldsymbol{\sigma}, \boldsymbol{\kappa}) = 0 \tag{1.5}$$

defines the boundary of the elastic domain. The evolution of plastic strains is defined by the flow rule which can be expressed as

$$\Delta\boldsymbol{\varepsilon}^{pl} = \Delta\lambda\, \boldsymbol{g} = \Delta\lambda \frac{\partial Q}{\partial \boldsymbol{\sigma}} \tag{1.6}$$

where $\Delta\boldsymbol{\varepsilon}^{pl}$ is the plastic strain increment, $\boldsymbol{g}$ is the flow direction, Q is the plastic potential, defining the direction of plastic strains, and $\Delta\lambda$ is the plastic multiplier increment, which controls the amount of plastic strains. In the special case of $Q{=}F$the flow rule is called associated. As a result, the plastic strains are perpendicular to the yield surface. Otherwise, $Q{\neq}F$, the flow rule is non-associated. This allows a more realistic representation of the effects that are known from experiments, e.g. dilatancy.

The plastic strain increases only if the material is in a plastic state, represented by Eq. (1.5). This condition can be expressed as

$$\Delta\lambda\, F = 0 \tag{1.7}$$

Furthermore, this condition implies that in an elastic state, cf. Eq. (1.4), the increment of the plastic multiplier is zero and the plastic strain remains constant. Since the flow rule defines the oriented direction of plastic strain evolution, the increment of plastic multiplier should not be negative

$$\Delta\lambda \geq 0 \tag{1.8}$$

Equations (1.3), (1.7) and (1.8) are known as Kuhn-Tucker (loading/unloading) conditions

$$F(\boldsymbol{\sigma}, \boldsymbol{\kappa}) \leq 0 \qquad \Delta\lambda\, F = 0 \qquad \Delta\lambda \geq 0 \tag{1.9}$$

Additionally, the consistency condition

$$\Delta\lambda\, \Delta F = 0 \tag{1.10}$$

expresses that during plastic flow the yield criterion must remain zero.

Finally, the evolution of the hardening/softening variables is given by the hardening/softening law which can be written as

$$\Delta\boldsymbol{\kappa} = \Delta\lambda \boldsymbol{h} \tag{1.11}$$

where $\boldsymbol{h}$ is the hardening/softening modulus. In general, the hardening/softening functions are used to describe the evolution of the yield surface while loading. For example, hardening results in an expansion of the yield-surface.

The implementation of plastic material models requires the solution of a nonlinear system of equations for the unknown stresses, plastic strains, and hardening/softening variables. Note that the flow rule and the hardening/softening rule relate the plastic strains and the hardening/softening variables to the plastic multiplier increment. As a result, the problem can be reduced to a single equation with unknown plastic multiplier.

The nonlinear equation is solved in an iterative way by incorporating the concept of linearization. Please note that this is an additional iterative procedure which is performed at the integration point (material point, Gauss point) level. At system level an iterative solution procedure, e.g. Newton-Raphson, needs to be applied because the global system of equations also become nonlinear, cf. Bathe [1].

It is assumed that all the variables of a previous step n are known. For a given strain increment $\boldsymbol{\Delta\varepsilon}^{\boldsymbol{tot}(\mathrm{n+1})}$ the unknowns are calculated in a two-step algorithm. In the first step, the elastic predictor step, a so-called trial stress is calculated (assuming that the plastic strains and the hardening/softening variables does not change)

$$\boldsymbol{\sigma}^{\boldsymbol{trial}} = \boldsymbol{C}\left[\boldsymbol{\varepsilon}^{\boldsymbol{tot}(n)} + \boldsymbol{\Delta\varepsilon}^{\boldsymbol{tot}(\mathrm{n+1})} - \boldsymbol{\varepsilon}^{\boldsymbol{pl}(n)}\right] \tag{1.12}$$

and the yield surface is evaluated. If

$$F(\boldsymbol{\sigma}^{\boldsymbol{trial}}, \boldsymbol{\kappa}^{(n)}) \leq 0 \tag{1.13}$$

the yield condition is satisfied, and the trial stress state is admissible. Consequently, the plastic strains and the hardening/softening variables do not develop in that step.

If

$$F\left(\boldsymbol{\sigma}^{\boldsymbol{trial}}, \boldsymbol{\kappa}^{(n)}\right) > 0 \tag{1.14}$$

the yield surface is violated, and the trial stress state is not admissible. As a result, in the second step, the plastic corrector step, the plastic multiplier is determined in an iterative procedure so that the stresses become admissible. As this is a plastic step, the stress state must be on the yield surface

$$F\left(\boldsymbol{\sigma}^{(n)}, \boldsymbol{\kappa}^{(n)}\right) = 0 \tag{1.15}$$

This step is often referred to as the return mapping because the trial stress is returned to the yield surface.

In multiPlas there are two return mapping algorithms, [9], [11], [12], [10] available – the cutting plane algorithm and the closest point projection. The algorithms differ in the assumption on the flow rule and hardening/softening rule during the iterative solution procedure.

In the cutting plane algorithm, the increments of the plastic strains and the increments of the hardening/softening variables are approximated by the explicit Euler forward method

$$\Delta\boldsymbol{\varepsilon}^{\boldsymbol{pl}(n+1)} = \Delta\lambda^{(\mathrm{n}+1)}\boldsymbol{g}^{(n)} \tag{1.16}$$

$$\Delta\boldsymbol{\kappa}^{(\mathrm{n}+1)} = \Delta\lambda^{(\mathrm{n}+1)}\,\boldsymbol{h}^{(n)} \tag{1.17}$$

Consequently, it is assumed that the direction of the plastic strains and the direction of the hardening/softening variables are constant during the time step. It is to be noted that this assumption might result in numerical problems during the return-mapping. In the implementation the directions are updated after each iteration step. But in the linearization of the governing equations, the derivatives of $\boldsymbol{g}$ and $\boldsymbol{h}$ with respect to the stresses and the hardening/softening variables are not considered. The advantage is that the numerical effort for the cutting plane algorithm is relatively small. Furthermore, this algorithm is very robust if the plastic potential is not smooth, e.g. Mohr-Coulomb criterion. The drawback is that because of the explicit approximation, this algorithm depends on the step size. For example, if the material softens then larger time steps generally result in a more brittle material behavior.

The second algorithm, the closest point projection, incorporates the implicit Euler backward approximation of the plastic strains and the hardening/softening variables

$$\Delta\boldsymbol{\varepsilon}^{\boldsymbol{pl}(n+1)} = \Delta\lambda^{(\mathrm{n}+1)}\boldsymbol{g}^{(n+1)} \tag{1.18}$$

$$\Delta\boldsymbol{\kappa}^{(\mathrm{n}+1)} = \Delta\lambda^{(\mathrm{n}+1)}\boldsymbol{h}^{(n+1)} \tag{1.19}$$

Consequently, the derivatives of $\boldsymbol{g}$ and $\boldsymbol{h}$ with respect to the stresses and the hardening/softening variables must be considered in the linearization of the governing equations. As a result, the algorithm becomes more complex and the numerical effort for solving the system of equations increases generally. The big advantage is that the closest point projection does not show any time dependency of the results. It is to be noted that this algorithm might fail if the plastic potential is not smooth.

1.1.2. Extension to multi-surface plasticity

In general, the failure of complex material cannot be described by a single yield-surface. The concept of multi-surface plasticity allows the incorporation of individual yield surfaces for the specific failure modes and failure mechanisms. The final yield surface is composed of the individual yield surfaces. As a result, the final multi-surface yield criterion is non-smooth in the stress domain. One requirement is that the final yield surface must be complex. Otherwise, the solution is not unique, and the return mapping algorithms might fail.

In the framework of multi-surface plasticity, the flow rule can be written as

$$\Delta\boldsymbol{\varepsilon}^{\boldsymbol{pl}} = \sum_{\alpha=1}^{n_{YC}} \Delta\lambda^{\alpha}\,\boldsymbol{g}^{\boldsymbol{\alpha}} = \sum_{\alpha=1}^{\mathrm{n_{YC}}} \Delta\lambda^{\alpha}\frac{\partial Q_{\alpha}}{\partial\boldsymbol{\sigma}} \tag{1.20}$$

and the hardening/softening rule reads

$$\Delta\boldsymbol{\kappa} = \sum_{\alpha=1}^{n_{YC}} \Delta\lambda^{\alpha}\,\boldsymbol{h}^{\boldsymbol{\alpha}} \tag{1.21}$$

where n_{YC} is the number of yield conditions. Every individual yield condition must satisfy the Kuhn-Tucker conditions

$$F_\alpha(\boldsymbol{\sigma}, \boldsymbol{\kappa}) \leq 0 \qquad \Delta\lambda^\alpha F_\alpha = 0 \qquad \Delta\lambda^\alpha \geq 0 \qquad \alpha = 1 \ldots n_{YC} \tag{1.22}$$

Consequently, in a plastic step all active yield functions must be zero

$$F_\alpha(\boldsymbol{\sigma}, \boldsymbol{\kappa}) = 0 \qquad \forall\alpha: F_\alpha \in \mathcal{J} \tag{1.23}$$

where $\mathcal{J}$ is the set of active yield surfaces. Generally, this non-linear system of equations is solved iteratively. The return mapping algorithms outlined in section 1.1, namely the cutting plane algorithm and the closest point projection, can be extended to the multi-surface plasticity [1].

In the numerical implementation, the algorithm has to deal with the singularities at the intersections between the different yield criteria (e.g. F_1 to F_2 as represented in Fig. 1-1). More than one yield criterion might be active simultaneously. This yields a system of equations for the corrections of plastic multipliers of active yield surfaces. Note that the number of active yield surface might be smaller than the total number of yield surfaces. The algorithm results in the plastic strains which return the stress to all the active yield surfaces. In the example in Fig. 1-1 the stress is returned to the intersection of F_1 and F_2 if both yield surfaces are active.

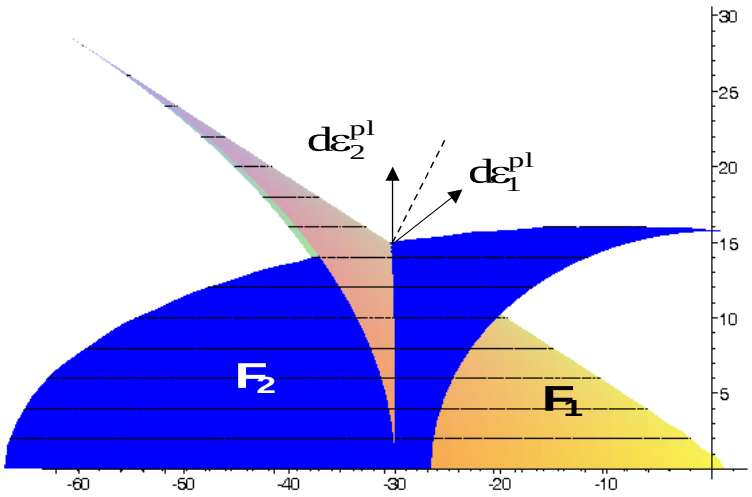

Fig. 1-1: Intersection between two flow criteria F1 and F2

In contrast to single surface plasticity exceeding the yield condition is no longer a sufficient criterion for activity of a yield criterion. Additionally, the corresponding plastic multiplier must be positive in one time step

$$\Delta\lambda^\alpha \geq 0 \qquad \alpha = 1 \ldots n_{YC} \tag{1.24}$$

Consequently, the activity might change during the return mapping because yield criteria might change depending on the hardening variables and the stresses. The consistent selection of active yield criterion ensures that the stress return within the intersection of yield surfaces is reasonable from a physical point of view.

1.2. Installation

Starting with the multiPlas release 5.8.0 for Ansys 2022 R1, the multiPlas library is fully integrated into Ansys. No further installation is required.

1.3. License

No additional multiPlas license is required. The multiPlas material models are available in following Ansys products:

- Enterprise
- PrepPost
- Solver

1.4. Model definition

multiPlas material models are defined by using the following APDL command:

TB, MULP, *mat*, …, 80

where *mat* is the material number and 80 is the number of material parameters. multiPlas material models assume a minimum size of 80 of the TBDATA-field, even if the specific material law has less than 80 parameters. Please do not change the size to a value less than 80. It is to be noted that some materials require more than 80 parameters.

The nonlinear material parameters of the multiPlas material model must be provided in this TBDATA-field. The corresponding material parameters written to the TBDATA-field by

TBDATA, 1, *LAW*, …, …,

where *LAW* is the multiPlas material identifier. All other material parameters depend on the specific material law.

Note: The TBDATA command allows the definition of 6 consecutive parameters. Additional parameters must be defined by executing the TBDATA command multiple times with different starting locations, cf. TBDATA description in the “Command Reference” of the Ansys “Mechanical APDL” documentation.

In addition, the number of state variables must be defined for the multiPlas material model using the following APDL command:

TB, STATE, *mat*, , *num_state_vars*

where *mat* is the material number and *num_state*_vars is the number of state variables. The number of state variables depends on the material model and is defined in the following sections.

Note: The multiPlas material data (**TB**, MULP and **TB**, STATE) cannot be defined in the “Engineering Data” of Ansys Workbench. But the material models can be used in “Mechanical Application” of Ansys Workbench. The models are directly defined in “Mechanical Application” by “Command Snippets”.

The linear elastic material properties (Young’s modulus, Poisson’s ratio, shear modulus) must be provided in the standard Ansys way. In Ansys mechanical APDL the linear elastic properties can be defined by following commands (assuming isotropic behavior):

EX, *mat*, *youngs_modulus*

NUXY, *mat*, *poisons_ratio*

Please refer to the Ansys manual for the full definition of an orthotropic material.

1.5. Update existing multiPlas material macros

The integrated version of multiPlas (since release 5.8 for Ansys 2022 R1) is using the same layout of material parameters as the standalone version (DLL or custom executable). As a result, existing multiPlas material macros can still be used. The following change in the material definition is necessary:

- The command **TB**, USER, … must be changed into **TB**, MULP, …

2. Material Models

In this section the material models (theory, input parameters and state variables) available in multiPlas are presented. The individual models are identified by the first entry in the TBDATA declaration (**TBDATA**, *1*, *LAW*). Table 2.1 summarizes the available material models.

Table 2.1: multiPlas material models

LAW	multiPlas material model
1	Sand model for casting simulation
17	Cast-Iron model with implicit creep
20	Masonry model with multi-linear softening
22	Masonry model with nonlinear softening
33	Wood model
34	Orthotropic boxed value model for additive manufacturing
141	Cable model
150	Laminated sheet package

The following system of units is used within this section:

- force: N
- length: m
- mass: kg
- time: s
- angles: ° (degrees)
- temperature: °C

This unit system can be converted into any other consistent unit system.

Note for workbench users: Please choose the correct unit system in Workbench. The Workbench unit system and the unit system of the multiPlas parameters must be identical. Otherwise, the simulation will most likely fail.

2.1. Sand model for casting simulation

This model is an extension of the jointed rock model (**TB**, JROCK) directly available in Ansys Geomechanical Toolbox. A detailed description of this model can be found in the "Material Reference" of the Ansys "Mechanical APDL" documentation.

The failure of jointed rock is represented by a combination of Mohr-Coulomb and Rankine (tension cut-off) yield surfaces. The material model differentiates between the anisotropic failure of one of the joint sets and the isotropic failure of intact rock (material between joints). Up to 4 independent joint sets can be defined.

As an additional feature, a permanent change of the material structure at a predefined temperature can be modeled, e.g. cohesive sand which becomes cohesionless during heating remains cohesionless during cooling. This feature is enabled by flag Tflag. In that case the maximum temperature during the simulation history is stored as additional history variable for any integration point. If that maximum temperature exceeds the limit temperature Tlimit, then the permanent change in material structure is assumed. If afterwards the temperature drops below the limit temperature, then the material parameters are evaluated at the limit temperature and not for the actual temperature.

The material model assumes ideal plastic behavior, but with residual strength parameters. Furthermore, the model allows a coupled reduction of tensile strength and of shear strength parameters for the individual material components (intact rock or joint set).

2.1.1. Material parameters

The material model is identified by LAW=1. The corresponding material parameters are summarized in Table 2.2.

Table 2.2: Sand model for casting simulation – parameters

	1	2	3	4	5	6	7	8	9	10
1-10 rock	**1**	φ_R	c_R	ψ_R	φ_R^*	c_R^*	$f_{t,R}$		$f_{t,R}^*$	njs
11-20 1st joint	φ_{J1}	c_{J1}	ψ_{J1}	φ_{J1}^*	c_{J1}^*	$f_{t,J1}$	α_{J1}	β_{J1}	$f_{t,J1}^*$	
21-30 2nd joint	φ_{J2}	c_{J2}	ψ_{J2}	φ_{J2}^*	c_{J2}^*	$f_{t,J2}$	α_{J2}	β_{J2}	$f_{t,J2}^*$	
31-40 3rd joint	φ_{J3}	c_{J3}	ψ_{J3}	φ_{J3}^*	c_{J3}^*	$f_{t,J3}$	α_{J3}	β_{J3}	$f_{t,J3}^*$	
41-50 4th joint	φ_{J4}	c_{J4}	ψ_{J4}	φ_{J4}^*	c_{J4}^*	$f_{t,J4}$	α_{J4}	β_{J4}	$f_{t,J4}^*$	
51-60										wr
61-70	Elem	Intpt	eps	geps	maxit	cutmax			algo	ktuser
71-80	T_{flag}	T_{limit}								rsc_flag

General parameters:

parameter	description	SI unit	range
njs	number of joint sets	[-]	0…4
rsc_flag	residual strength coupling flag 0 – coupling is disabled 1 – coupling is enabled for joint sets 2 – coupling is enabled for intact rock 3 – coupling is enabled for both	[-]	0…3

parameter	description	SI unit	range
T_{flag}	flag considering a permanent change in material structure at a predefined temperature 0 – disabled 1 – enabled	[-]	0,1
T_{limit}	temperature at which the permanent change in material structure takes place	[°C]	

Intact rock (base material between the joint sets) parameters:

- parameters of the isotropic Mohr-Coulomb yield surface:

parameter	description	SI unit	range
φ_R	initial friction angle	[°]	$0° \leq \varphi_R < 90°$
c_R	initial cohesion	[N/m²]	$c_R \geq 0$
ψ_R	dilatancy angle	[°]	$0° \leq \psi_R \leq \varphi_R$
φ_R^*	residual friction angle	[°]	$0° \leq \varphi_R^* \leq \varphi_R$
c_R^*	residual cohesion	[N/m²]	$0 \leq c_R^* \leq c_R$

- parameters of the isotropic Rankine (tension cut-off) yield surface:

parameter	description	SI unit	range
$f_{t,R}$	initial uniaxial tensile strength	[N/m²]	$f_{t,R} > 0$
$f_{t,R}^*$	residual uniaxial tensile strength	[N/m²]	$0 < f_{t,R}^* \leq f_{t,R}$

Note: The Rankine yield surface is only active if $\varphi_R = 0°$ or $f_{t,R} < \frac{c_R}{\tan \varphi_R}$.

Joint material parameters (up to 4 joint sets can be defined)

- parameters of the anisotropic Mohr-Coulomb yield surface:

parameter	description	SI unit	range
φ_{Ji}	initial friction angle of joint *i*	[°]	$0° \leq \varphi_{Ji} < 90°$
c_{Ji}	initial cohesion of joint *i*	[N/m²]	$c_{Ji} \geq 0$
ψ_{Ji}	dilatancy angle of joint *i*	[°]	$0° \leq \psi_{Ji} \leq \varphi_{Ji}$
φ_{Ji}^*	residual friction angle of joint *i*	[°]	$0° \leq \varphi_{Ji}^* \leq \varphi_{Ji}$
c_{Ji}^*	residual cohesion of joint *i*	[N/m²]	$0 \leq c_{Ji}^* \leq c_{Ji}$

- parameters of the anisotropic tension cut-off yield surface:

parameter	description	SI unit	range
$f_{t,Ji}$	initial uniaxial tensile strength of joint *i*	[N/m²]	$f_{t,Ji} > 0$
$f_{t,Ji}^*$	residual uniaxial tensile strength of joint *i*	[N/m²]	$0 < f_{t,Ji}^* \leq f_{t,Ji}$

Note: The tension cut-off yield surface is only active if $\varphi_{Ji} = 0°$ or $f_{t,Ji} < \frac{c_{Ji}}{\tan \varphi_{Ji}}$.

- direction of anisotropic joint system:

parameter	description	SI unit	range
α_{Ji}	negative rotation about element Z-axis (joint *i*)	[°]	
β_{Ji}	positive rotation about new Y-axis (joint *i*)	[°]	

2.1.2. State variables

This model defines a variable number of state variables which depends on the number of joint sets, njs, and the parameter T_{flag}. The actual number of state variables can be calculated as 3+3*njs+T_{flag}. The state variables are summarized in Table 2.3.

Table 2.3: Sand model for casting simulation – state variables

state variable	description
1	number representing the activity of individual yield surfaces (failure modes)
2	accumulated plastic multiplier of the isotropic Mohr-Coulomb yield surface

state variable	description
3	accumulated plastic multiplier of the isotropic Rankine yield surface
3 + 3 * (*i* - 1) + 1	accumulated tangential plastic strains due to Mohr-Coulomb failure of joint *i*
3 + 3 * (*i* - 1) + 2	accumulated normal plastic strains due to Mohr-Coulomb failure of joint *i*
3 + 3 * (*i* - 1) + 3	accumulated normal plastic strains due to tensile failure of joint *i*
3 + 3 * njs + T_{flag}	maximum temperature during simulation history of the integration point

2.1.3. Activity encoding

The activity of individual yield surface is encoded into a single number. The following table shows the encoding if a single yield surface fails. If multiple yield surfaces fail then the corresponding numbers are added, e.g. 11 represents shear failure of intact rock and joint 1.

number	activity
1	shear failure (Mohr-Coulomb yield surface) of intact rock
10	shear failure (Mohr-Coulomb yield surface) of joint 1
100	shear failure (Mohr-Coulomb yield surface) of joint 2
1 000	shear failure (Mohr-Coulomb yield surface) of joint 3
10 000	shear failure (Mohr-Coulomb yield surface) of joint 4
100 000	tensile failure (Rankine yield surface) of intact rock
1 000 000	tensile failure (tension cut-off yield surface) of joint 1
10 000 000	tensile failure (tension cut-off yield surface) of joint 2
100 000 000	tensile failure (tension cut-off yield surface) of joint 3
1 000 000 000	tensile failure (tension cut-off yield surface) of joint 4

2.2. Cast iron model with implicit creep

The failure of cast iron is represented by a combination of von-Mises and Rankine yield surfaces. The material model is based on the Ansys cast iron model. In contrast to the Ansys cast iron model, the multi-surface plasticity framework is used, a rounded Rankine criterion is applied and the plastic potential in compression (von Mises yield-surface) is slightly modified (associative flow). Furthermore, the model can be combined with implicit creep.

2.2.1. Material parameters

The multiPlas cast iron model is selected by setting Law=17. The corresponding material parameters are summarized in Table 2.4.

Table 2.4: Cast iron creep model – parameters

	1	2	3	4	5	6	7	8	9	10
1-10	**17**	σ_{Yt}	σ_{Yc}	ν_{pl}	α	flag				
11-20	$\kappa_{t,1}$	$\kappa_{t,2}$	$\kappa_{t,3}$	$\kappa_{t,4}$	$\kappa_{t,5}$	$\kappa_{t,6}$	$\kappa_{t,7}$	$\kappa_{t,8}$	$\kappa_{t,9}$	$\kappa_{t,10}$
21-30	$\Omega_{t,1}$	$\Omega_{t,2}$	$\Omega_{t,3}$	$\Omega_{t,4}$	$\Omega_{t,5}$	$\Omega_{t,6}$	$\Omega_{t,7}$	$\Omega_{t,8}$	$\Omega_{t,9}$	$\Omega_{t,10}$
31-40	$\kappa_{c,1}$	$\kappa_{c,2}$	$\kappa_{c,3}$	$\kappa_{c,4}$	$\kappa_{c,5}$	$\kappa_{c,6}$	$\kappa_{c,7}$	$\kappa_{c,8}$	$\kappa_{c,9}$	$\kappa_{c,10}$
41-50	$\Omega_{c,1}$	$\Omega_{c,2}$	$\Omega_{c,3}$	$\Omega_{c,4}$	$\Omega_{c,5}$	$\Omega_{c,6}$	$\Omega_{c,7}$	$\Omega_{c,8}$	$\Omega_{c,9}$	$\Omega_{c,10}$
51-60										wr
61-70	Elem	Intpt	eps	geps	maxit	cutmax			algo	ktuser
71-80										
81-90	claw	c_1	c_2	c_3	c_4	c_5	c_6	c_7	c_8	c_9
91-100	c_{10}	c_{11}	c_{12}	c_{13}	c_{14}	c_{15}	c_{16}	c_{17}	c_{18}	T_{offset}

Base parameters:

parameter	description	SI unit	range
σ_{Yt}	uni-axial tensile strength ($\kappa_t = 0$)	[Pa]	$\sigma_{Yt} > 0$
σ_{Yc}	uni-axial compressive strength ($\kappa_c = 0$)	[Pa]	$\sigma_{Yc} > 0$
ν_{pl}	plastic Poisson's ratio	[-]	$-1 < \nu_{pl} < 0.5$
α	Rankine yield surface rounding factor the rounding radius is $r = \alpha \cdot \sigma_{Yt}$ $\alpha = 0$: no rounding $\alpha = 1$: full tensile rounding	[-]	$0 \leq \alpha \leq 1$
flag	check yield surface in first Newton-Raphson iteration (might help convergence in cooling problems) flag=0: yield surfaces are evaluated for all steps flag=1: yield surfaces are not evaluated in first equilibrium iteration step feature is only available in custom executable	[-]	0,1

Isotropic hardening/softening parameters:

parameter	description	SI unit	range
$\kappa_{t,i}$	equivalent plastic strain in tension at point i (i=1…10), for the multi-linear definition of the stress-strain relationship, the plastic strains must be defined in increasing order (if the plastic strain is lower than the previous one, then this point and all the following points are ignored)	[-]	$\kappa_{t,0}=0$ $\kappa_{t,(i-1)} < \kappa_{t,i}$
$\Omega_{t,i}$	relative tensile strength at point i (i=1…10)	[-]	$\Omega_{t,0} = 1$ $\Omega_{t,i} > 0$

parameter	description	SI unit	range
$\kappa_{c,i}$	equivalent plastic strain in compression at point i (i=1…10), for the multi-linear definition of the stress-strain relationship, the plastic strains must be defined in increasing order (if the plastic strain is lower than the previous one, then this point and all the following points are ignored)	[-]	$\kappa_{c,0}=0$ $\kappa_{c,(i-1)} < \kappa_{c,i}$
$\Omega_{c,i}$	relative compressive strength at point i (i=1…10)	[-]	$\Omega_{c,0} = 1$ $\Omega_{c,i} > 0$

Creep parameters:

The creep parameters are explained in Section 2.8.

2.2.2. State variables

In this model **10** state variables are defined. The state variables are summarized inTable 2.5.

Table 2.5: Cast iron creep model – state variables

state variable	description
1	number representing the activity of individual yield surfaces (failure modes)
2	hardening variable (equivalent plastic strain) in tension (Rankine)
3	hardening variable (equivalent plastic strain) in compression (von Mises)
4	Creep strain in x direction
5	Creep strain in y direction
6	Creep strain in z direction
7	Creep strain in xy direction
8	Creep strain in yz direction
9	Creep strain in xz direction
10	Accumulated creep strain $\int_0^t \dot{\varepsilon_{cr}} dt$

2.2.3. Activity encoding

The activity of individual yield surface is encoded into a single number. The following table shows the encoding if a single yield surface fails. If multiple yield surfaces fail then the corresponding numbers are added, e.g. 11 represents of both yield surfaces.

number	activity
1	Rankine – tensile failure
10	von Mises – compressive failure

2.3. Masonry

The orthotropic strength of a regular masonry is modeled by an extended spatial masonry model which is based on the Ganz yield criterion [9], [4]. The Ganz model is the foundation of the Swiss masonry norm SIA 177/2 and complies with the fracturing model of Mann [6] which is contained in German standard DIN 1053 as well as with the natural stone masonry model suggested by Berndt [3]. In the Ganz masonry model, an additional interaction with a horizontal load (parallel to the longitudinal joint) is considered. The necessary material parameters of this model are compression- and tensile strength of the masonry, the friction angle, and the cohesion between brick and joint as well as the brick dimensions. The multi-surface yield condition, shown in Fig. 2-1, represents the different failure mechanisms of regular masonry formation. The individual yield criteria are given in Table 2.6.

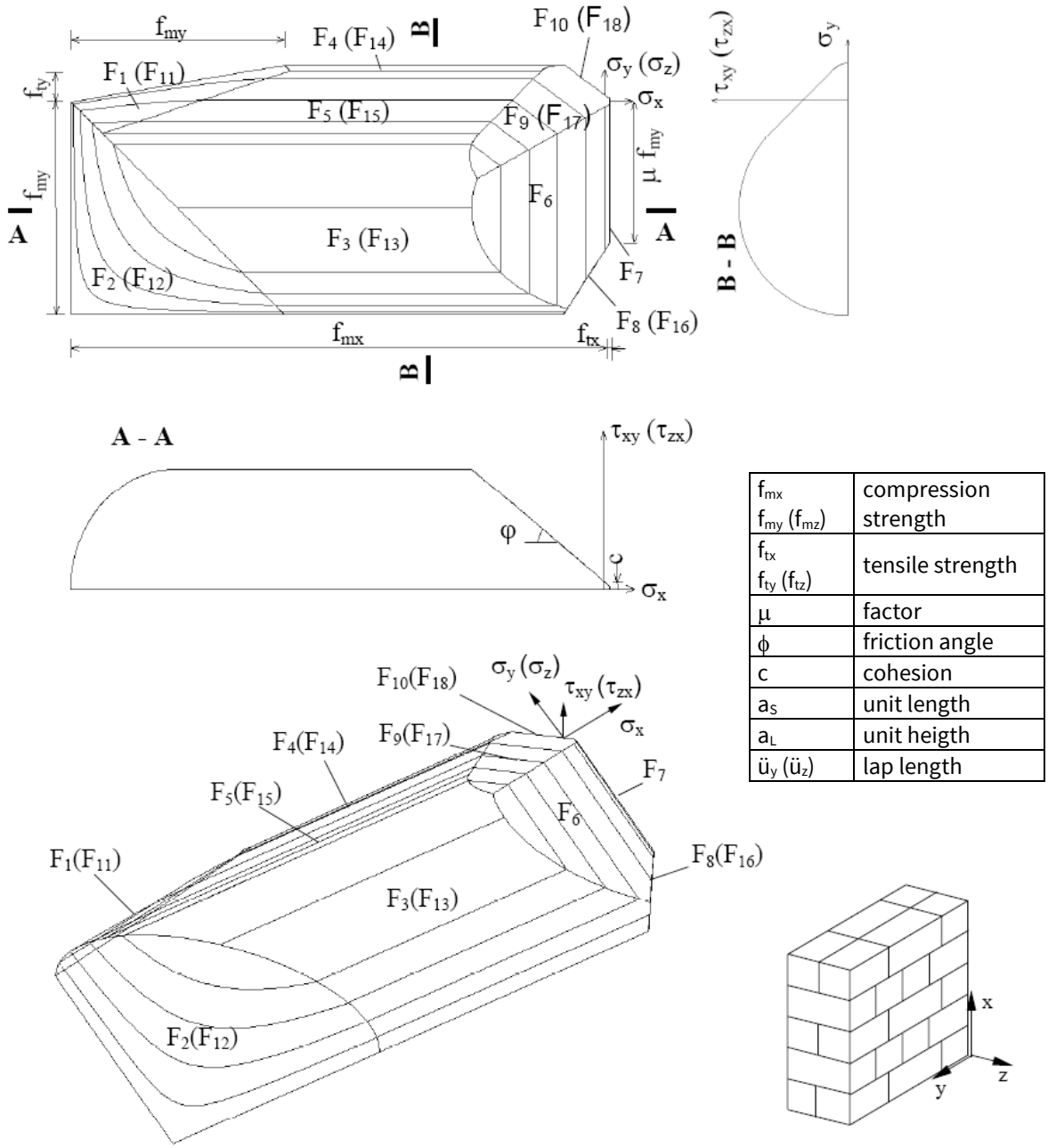

f_{mx} f_{my} (f_{mz})	compression strength
f_{tx} f_{ty} (f_{tz})	tensile strength
μ	factor
ϕ	friction angle
c	cohesion
a_S	unit length
a_L	unit heigth
$ü_y$ ($ü_z$)	lap length

Fig. 2-1: Ganz material model for masonry [9]

Table 2.6: Masonry model – yield functions

yield function	failure mechanism
F1 (F11)	tensile failure of brick
F2 (F12)	compressive failure of masonry
F3 (F13)	shear failure of masonry (brick failure)
F4 (F14)	tensile failure parallel to bed joint (brick failure)
F5 (F15)	shear failure of masonry
F6	shear failure of bed joint
F7	tensile failure of bed joint
F8 (F16)	tensile failure of bed joint under high horizontal pressure
F9 (F17)	staircase-shaped shear failure
F10 (F18)	tensile failure of masonry parallel to bed joints (joint failure)

The orthotropic nonlinear stress-strain behavior of masonry is described using the corresponding softening and hardening models [9].

2.3.1. Nonlinear stress-strain relation for compressive failure

In multiPlas the nonlinear stress-strain relationship in compression can be described by two different models. Fig. 2-2 shows the corresponding uniaxial stress strain curves.

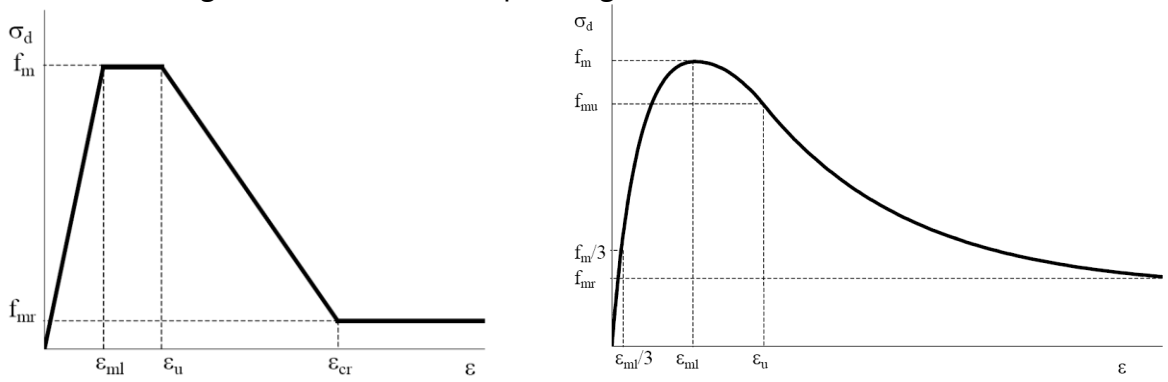

multiPlas law 20 multiPlas law 22

Fig. 2-2: Masonry model – uniaxial stress-strain relationship of masonry in compression.

In multiPlas law 22 a combination of a parabolic hardening/softening function and an exponential softening function, which is based on the German standard DIN 1045-1, is applied. multiPlas law 20 uses a simplified multi-linear softening model. The simplified model is often sufficiently accurate for practical applications.

2.3.2. Nonlinear stress-strain relation for tensile failure perpendicular to the bed joints

The material behavior perpendicular to the bed joints in tension is described by an exponential softening function. Fig. 2-3 shows the corresponding uniaxial stress-strain curve. To overcome spurious mesh dependency due to softening and localization, a regularization of the fracture energy with respect to an equivalent element length is applied. This approach is based on the crack band theory of Bažant and Oh [2]. The equivalent element length is calculated according to Poelling [8].

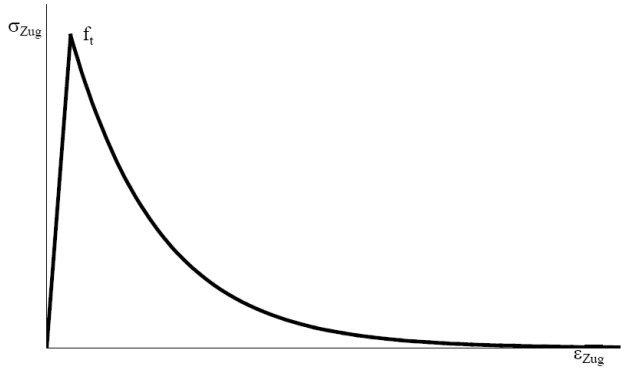

Fig. 2-3: Masonry model – stress-strain relation under tensile load perpendicular to the bed joints

2.3.3. Nonlinear stress-strain relation for shear failure of bed joints

Shear failure of the bed joints, which can be observed in experiments, can be described by an exponential degradation of the cohesion *c* and linear reduction of the initial friction angle ϕ_o to a residual friction angle ϕ_R. Fig. 2-4 shows the corresponding stress-strain curve. The softening model for cohesion *c* is based on the fracture energy approach described in the previous section. It is assumed that the cohesion diminishes completely if the area specific mode-II fracture energy G^{II}_{fJ} (mode II – adhesion-shear-strength) is dissipated. This has been experimentally established by van der Pluijm [7]. The softening functions for tensile failure and shear failure are synchronized.

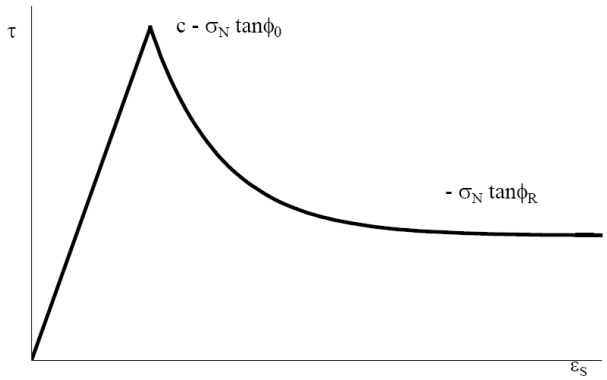

Fig. 2-4: Masonry model – nonlinear stress-strain relation in case of shear of bed joint

2.3.4. Material parameters - multi-linear softening (Law 20)

In law 20 the hardening/softening behavior of masonry in compression is described by simplified multi-linear functions. Fig. 2-5 shows the uniaxial stress-strain curve in compression and the corresponding softening function. The softening behavior for tensile and shear failure is represented by the fracture energy based exponential softening functions, cf Fig. 2-6. The corresponding material parameters are summarized in Table 2.7.

Table 2.7: Masonry model with multi-linear hardening/softening – parameters

	1	2	3	4	5	6	7	8	9	10
1-10	**20**	f_{mx}	f_{my}	f_{tx}	f_{txx}	f_{ty}	ζ_y	κ_u	Ω_r	as_y
11-20	al	$\ddot{u}_y$	ϕ	c	ϕ_r	ψ	direc	dreid	f_{mz}	f_{tz}
21-30	f_{tzz}	ζ_z	as_z	$\ddot{u}_z$						
31-40										
41-50										
51-60	G^{I}_{FJ}	G^{I}_{FB}	G^{II}_{FJ}	G_m		c_r	f_{tr}	ψ_r		wr
61-70	Elem	Intpt	eps	geps	maxit	cutmax			algo	ktuser
71-80										

Strength parameters:

- compressive strength parameters

parameter	description	SI unit	range
f_{mx}	uniaxial compressive strength of masonry normal to bed joints	[N/m^2]	$f_{mx} > 0$
f_{my}	uniaxial compressive strength of masonry normal to head joints	[N/m^2]	$0 < f_{my} \le f_{mx}$
ζ_y	factor scaling the compressive strength normal to head joints in yield function F_8	[-]	$\zeta_y > 0$
f_{mz}	uniaxial compressive strength of masonry normal to longitudinal joints	[N/m^2]	$f_{mz} > 0$
ζ_z	factor scaling the compressive strength normal to longitudinal joints in yield function F_{16}	[-]	$\zeta_z > 0$
κ_u	hardening/softening variable (plastic strain) defining start of linear softening	[-]	$\kappa_u > 0$
Ω_r	residual relative compressive strength	[-]	$0 < \Omega_r \le 1$
G_m	area specific "strain energy" for compressive failure	[Nm/m^2]	$G_m > 0$

- shear strength parameters

parameter	description	SI unit	range
c	cohesion of bed joints	[N/m^2]	$c > 0$
c_r	residual cohesion of bed joints	[N/m^2]	$0 < c_r \le c$
ϕ	friction angle of bed joints	[°]	$0° < \phi < 90°$
ϕ_r	residual friction angle of bed joints	[°]	$0° < \phi_r \le \phi$
ψ	dilatancy angle of bed joints	[°]	$0° < \psi \le \phi$
ψ_r	residual dilatancy angle of bed joints	[°]	$0° < \psi_r \le \psi$
G^{II}_{FJ}	area specific mode-II fracture energy of bed joints	[Nm/m^2]	$G^{II}_{FJ} > 0$

- tensile strength parameters

parameter	description	SI unit	range
f_{tx}	uniaxial tensile strength of masonry normal to bed joints	[N/m^2]	$f_{tx} > 0$
f_{ty}	uniaxial tensile strength of masonry normal to head joints	[N/m^2]	$f_{ty} > 0$
f_{tz}	uniaxial tensile strength of masonry normal to longitudinal joints	[N/m^2]	$f_{tz} > 0$
f_{tr}	residual tensile strength	[N/m^2]	$0 < f_{tr} \le \min(f_{tx}, f_{ty}, f_{tz})$
G^{I}_{FJ}	area specific mode-I fracture energy of bed joints	[Nm/m^2]	$G^{I}_{FJ} > 0$
G^{I}_{FB}	area specific mode-I fracture energy of stone	[Nm/m^2]	$G^{I}_{FB} > 0$

Geometrical parameters:

parameter	description	SI unit	range
f_{txx}	geometrical parameter in yield function F_8	[N/m^2]	$f_{txx} > 0$
f_{tzz}	geometrical parameter in yield function F_{16}	[N/m^2]	$f_{txx} > 0$
as_y	mean distance between head joints	[m]	$as_y > 0$
as_z	mean distance between longitudinal joints	[m]	$as_z > 0$
al	mean distance between bed joints	[m]	$al > 0$
$ü_y$	head joints overlap	[m]	$ü_y \ge 0$
$ü_z$	longitudinal joints overlap	[m]	$ü_z \ge 0$

Control parameters:

parameter	description	SI unit	range
direc	orientation of the joints relative to the element coordinate system, cf. Table 2.8	[-]	0, 1, 2

parameter	description	SI unit	range
dreid	strength monitoring flag: 0 - 2D monitoring (F_1 to F_{10}) 1 - 2.5D monitoring (F_1 to F_{10} and F_6 with τ_{res}) 2 - 3D monitoring (F_1 to F_{10})	[-]	0, 1, 2

Note: All fracture energies are regularized with respect to the element length.

Table 2.8: Masonry model – definition of control parameter direc.

direc	x-axis	y-axis	z-axis
0	normal to bed joint	normal to head joint	normal to longitudinal joint
1	normal to longitudinal joint	normal to head joint	normal to bed joint
2	normal to head joint	normal to bed joint	normal to longitudinal joint

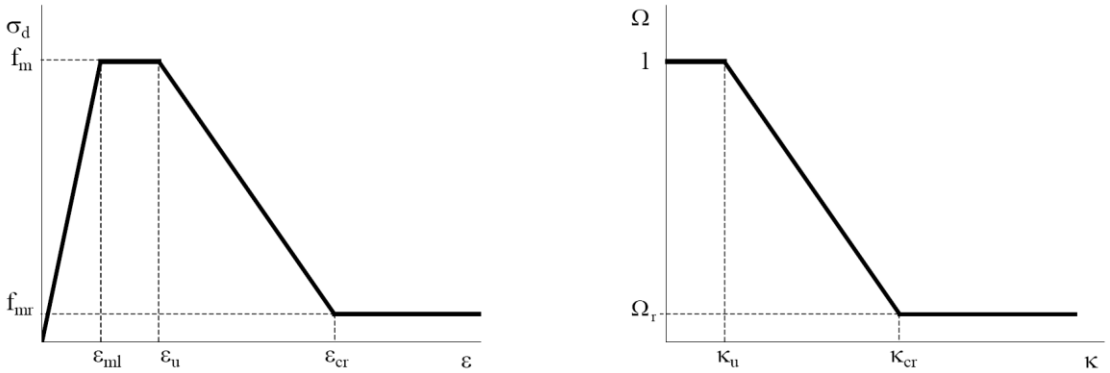

uniaxial stress-strain relationship in compression — softening model

Fig. 2-5: Law 20: uniaxial stress-strain curve of masonry in compression

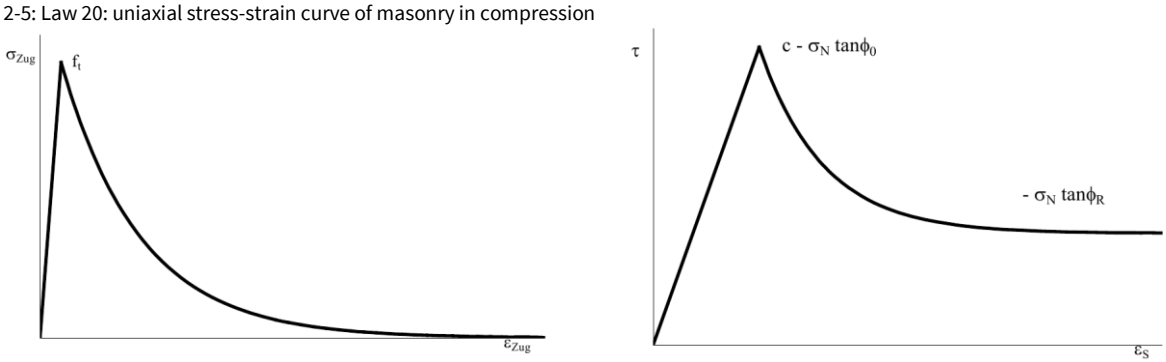

uniaxial stress-strain relationship in tension — stress-strain relationship of bed joints (shear)

Fig. 2-6: Law 20/Law 22: stress-strain curves for tensile and shear loading

2.3.5. Material parameters - nonlinear softening (Law 22)

In law 22 the hardening/softening behavior of masonry in compression is described by a combination of a parabolic hardening/softening function and an exponential softening function. Fig. 2-7 shows the uniaxial stress-strain curve in compression. The softening behavior for tensile and shear failure is represented in the same way as in law 20 by fracture energy based exponential softening functions, cf Fig. 2-6. The corresponding material parameters are summarized in Table 2.9.

Table 2.9: Masonry model with nonlinear hardening/softening – parameters

	1	2	3	4	5	6	7	8	9	10
1-10	**22**	f_{mx}	f_{my}	f_{tx}	f_{txx}	f_{ty}	ζ_y	κ_{ml}	Ω_r	as_y
11-20	al	$\ddot{u}_y$	ϕ	c	ϕ_r	ψ	direc	dreid	f_{mz}	f_{tz}
21-30	f_{tzz}	ζ_z	as_z	$\ddot{u}_z$		κ_{cu}				
31-40										
41-50										
51-60	G^I_{FJ}	G^I_{FB}	G^{II}_{FJ}			c_r	f_{tr}	ψ_r		wr
61-70	Elem	Intpt	eps	geps	maxit	cutmax			algo	ktuser
71-80										

Strength parameters:

- compressive strength parameters

parameter	description	SI unit	range
f_{mx}	uniaxial compressive strength of masonry normal to bed joints	[N/m²]	$f_{mx} > 0$
f_{my}	uniaxial compressive strength of masonry normal to head joints	[N/m²]	$0 < f_{my} \leq f_{mx}$
ζ_y	factor scaling the compressive strength normal to head joints in yield function F_8	[-]	$\zeta_y > 0$
f_{mz}	uniaxial compressive strength of masonry normal to longitudinal joints	[N/m²]	$f_{mz} > 0$
ζ_z	factor scaling the compressive strength normal to longitudinal joints in yield function F_{16}	[-]	$\zeta_z > 0$
κ_{ml}	hardening/softening variable (plastic strain) at compressive strength	[-]	$\kappa_{ml} > 0$
κ_{cu}	hardening/softening variable (plastic strain) at 85% of compressive strength (post peak)	[-]	$\kappa_{cu} > \kappa_{ml}$
Ω_r	residual relative compressive strength	[-]	$0 < \Omega_r \leq 0.85$

- shear strength parameters

parameter	description	SI unit	range
c	cohesion of bed joints	[N/m²]	$c > 0$
c_r	residual cohesion of bed joints	[N/m²]	$0 < c_r \leq c$
ϕ	friction angle of bed joints	[°]	$0° < \phi < 90°$
ϕ_r	residual friction angle of bed joints	[°]	$0° < \phi_r \leq \phi$
ψ	dilatancy angle of bed joints	[°]	$0° < \psi \leq \phi$
ψ_r	residual dilatancy angle of bed joints	[°]	$0° < \psi_r \leq \psi$
G^{II}_{FJ}	area specific mode-II fracture energy of bed joints	[Nm/m²]	$G^{II}_{FJ} > 0$

- tensile strength parameters

parameter	description	SI unit	range
f_{tx}	uniaxial tensile strength of masonry normal to bed joints	[N/m²]	$f_{tx} > 0$
f_{ty}	uniaxial tensile strength of masonry normal to head joints	[N/m²]	$f_{ty} > 0$
f_{tz}	uniaxial tensile strength of masonry normal to longitudinal joints	[N/m²]	$f_{tz} > 0$
f_{tr}	residual tensile strength	[N/m²]	$0 < f_{tr} \leq \min(f_{tx}, f_{ty}, f_{tz})$
G^I_{FJ}	area specific mode-I fracture energy of bed joints	[Nm/m²]	$G^I_{FJ} > 0$
G^I_{FB}	area specific mode-I fracture energy of stone	[Nm/m²]	$G^I_{FB} > 0$

Geometrical parameters:

parameter	description	SI unit	range
f_{txx}	geometrical parameter in yield function F_8	[N/m²]	$f_{txx} > 0$
f_{tzz}	geometrical parameter in yield function F_{16}	[N/m²]	$f_{txx} > 0$

parameter	description	SI unit	range
as_y	mean distance between head joints	[m]	$as_y > 0$
as_z	mean distance between longitudinal joints	[m]	$as_z > 0$
al	mean distance between bed joints	[m]	al > 0
$ü_y$	head joints overlap	[m]	$ü_y \geq 0$
$ü_z$	longitudinal joints overlap	[m]	$ü_z \geq 0$

Control parameters:

parameter	description	SI unit	range
direc	orientation of the joints relative to the element coordinate system, cf. Table 2.8	[-]	0, 1, 2
dreid	strength monitoring flag: 0 - 2D monitoring (F_1 to F_{10}) 1 - 2.5D monitoring (F_1 to F_{10} and F_6 with τ_{res}) 2 - 3D monitoring (F_1 to F_{10})	[-]	0, 1, 2

Note: All fracture energies are regularized with respect to the element length.

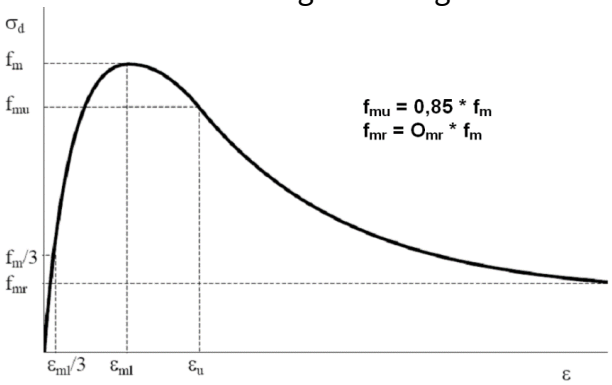

Fig. 2-7: Masonry model with nonlinear hardening/softening: uniaxial stress-strain curve of masonry in compression

2.3.6. State variables

In this model **14** state variables are defined, cf. Table 2.10.

Table 2.10: Masonry model (law 20/22) – state variables

state variable	description
1	number representing the activity of individual yield surfaces (failure modes)
2	hardening variable for tensile failure perpendicular to bed joint
3	first part of hardening variable for tensile failure perpendicular to head joint
4	second part of hardening variable for tensile failure perpendicular to head joint
5	first part of hardening variable for tensile failure perpendicular to longitudinal joint
6	second part of hardening variable for tensile failure perpendicular to longitudinal joint
7	first part of hardening variable for shear failure of bed joint
8	second part of hardening variable for shear failure of bed joint
9	hardening variable for compressive failure
10	hardening variable for tensile failure perpendicular to head joint
11	hardening variable for tensile failure perpendicular to longitudinal joint
12	hardening variable for shear failure of bed joint
13	hardening variable for dilatancy angel of bed joint
14	tan dilatancy angle of bed joint

2.3.7. Activity encoding

The activity of the individual yield surfaces is encoded into a single number. The following table shows the encoding if a single yield surface fails. If multiple yield surfaces fail, then the corresponding numbers are added.

number	activity
1	yield surface F_1 or F_{11}
10	yield surface F_2 or F_{12}
100	yield surface F_3 or F_{13}
1 000	yield surface F4 or F_{14}
10 000	yield surface F_5 or F_{15}
100 000	yield surface F_6
1 000 000	yield surface F_7
10 000 000	yield surface F_8 or F_{16}
100 000 000	yield surface F_9 or F_{17}
1 000 000 000	yield surface F_{10} or F_{18}

2.4. Wood

The wood material model is based on the boxed-value approach described in Grosse [5]. In multiPlas the orthotropic boxed value model is implemented within the framework of multi-surface plasticity in law 33. This law considers the interaction between longitudinal, radial, and tangential material behavior of wood. Fig. 2-8 and Fig. 2-9 show the individual yield surfaces.

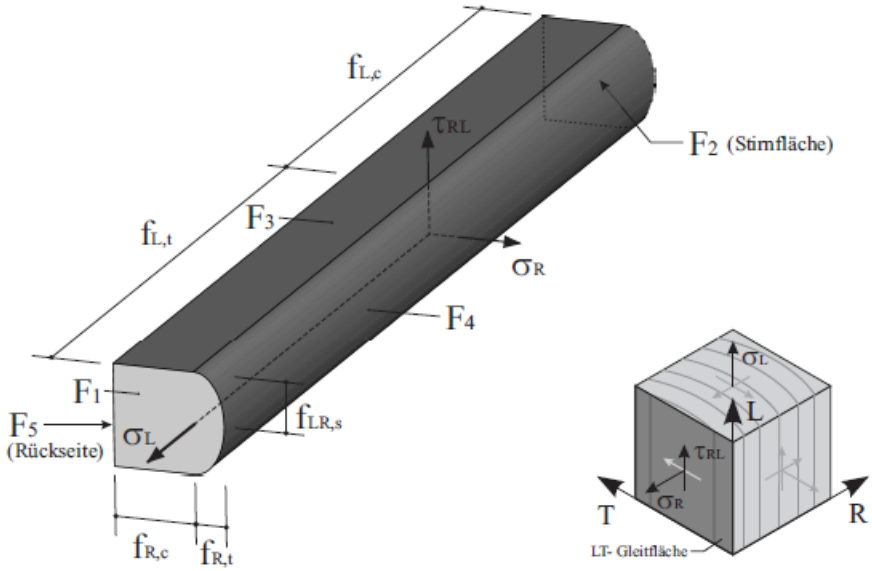

Fig. 2-8: Wood yield surfaces – interaction longitudinal vs. radial

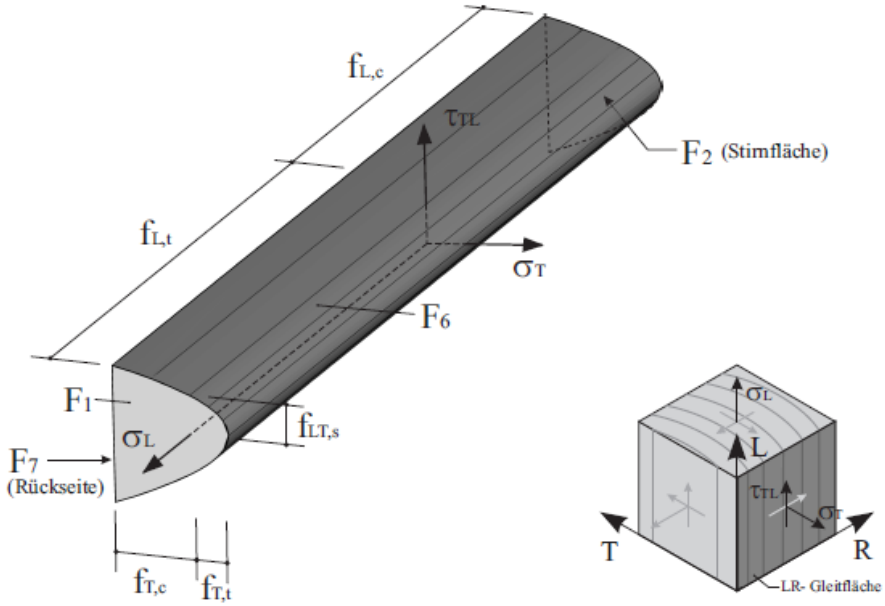

Fig. 2-9: Wood yield surfaces – interaction longitudinal vs. tangential

In multiPlas, the following coordinate system convention is assumed for the orientation of wood fibers:

- radial direction: element coordinate system x-axis
- tangential direction: element coordinate system y-axis
- longitudinal direction: element coordinate system z-axis

This convention holds for cartesian and cylindrical coordinate systems.

The individual yield functions are shortly summarized as follows. A more detailed description can be found in [5].

The first yield surface describes the fiber rupture (tensile failure in longitudinal direction)

$$F_1 = \sigma_{LL} - f_{Lt}\Omega_{Lt} = 0 \tag{2.1}$$

where f_{Lt} is the uniaxial tensile strength in longitudinal direction and Ω_{Lt} is the corresponding hardening/softening function.

The yield function for the compressive failure in longitudinal direction (fiber compression) is given by

$$F_2 = -\sigma_{LL} - f_{Lc}\,\Omega_{Lc} = 0 \tag{2.2}$$

where f_{Lc} is the uniaxial compressive strength in longitudinal direction and Ω_{Lc} is the corresponding hardening/softening function.

The third yield surface represents the initiation and the evolution of cracks parallel to the LT-plane

$$F_3 = \left(\frac{\langle\sigma_{RR}\rangle}{f_{Rt}\Omega_{Rt}}\right)^2 + \left(\frac{\sigma_{RL}}{f_{RLs}\Omega_{RLs}}\right)^2 + \left(\frac{\sigma_{RT}}{f_{RTs}\Omega_{RTs}}\right)^2 - 1 = 0 \tag{2.3}$$

with

$$\langle\sigma_{RR}\rangle = \begin{cases} 0 & \sigma_{RR} \le 0 \\ \sigma_{RR} & \sigma_{RR} > 0 \end{cases}$$

where f_{Rt} is the uniaxial tensile strength in radial direction, f_{RLs} is the radial/longitudinal shear strength, f_{RTs} is the radial/tangential shear strength and Ω_{Rt}, Ω_{RLs}, Ω_{RTs} are the corresponding hardening/softening functions.

The yield surface for the radial compressive failure (radial fiber compression) can be written as

$$F_4 = -\sigma_{RR} - f_{Rc}\Omega_{Rc} = 0 \tag{2.4}$$

where f_{Rc} is the uniaxial compressive strength in radial direction and Ω_{Rc} is the corresponding hardening/softening function.

The initiation and the evolution of cracks parallel to the LR-plane is described by the following yield surface

$$F_5 = \frac{\sigma_{TT}}{f_{Tt}\Omega_{Tt}} + \left(\frac{\sigma_{TR}}{f_{TRs}\Omega_{TRs}}\right)^2 + \left(\frac{\sigma_{TL}}{f_{TLs}\Omega_{TLs}}\right)^2 - 1 = 0, \tag{2.5}$$

where f_{Tt} is the uniaxial tensile strength in radial direction, f_{TRs} is the tangential/radial shear strength, f_{TLs} is the tangential/longitudinal shear strength and Ω_{Tt}, Ω_{TRs}, Ω_{TLs} are the corresponding hardening/softening functions.

Finally, the yield surface representing the compressive failure in tangential direction (tangential fiber compression) is given by

Tangential Compression of fiber

$$F_6 = -\sigma_{TT} - f_{Tc}\Omega_{Tc} = 0 \tag{2.6}$$

where f_{Tc} is the uniaxial compressive strength in tangential direction and Ω_{Tc} is the corresponding hardening/softening function.

Fig. 2-10**,** Fig. 2-11 and Fig. 2-12 illustrate the non-linear hardening/softening functions (in terms of uniaxial stress-strain curves) for the individual failure mechanisms.

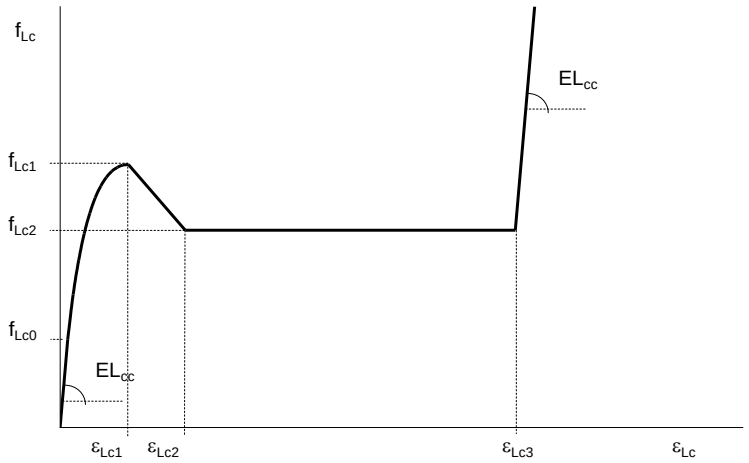

Fig. 2-10: Wood model – uniaxial stress-strain curve in longitudinal compression (fiber direction)

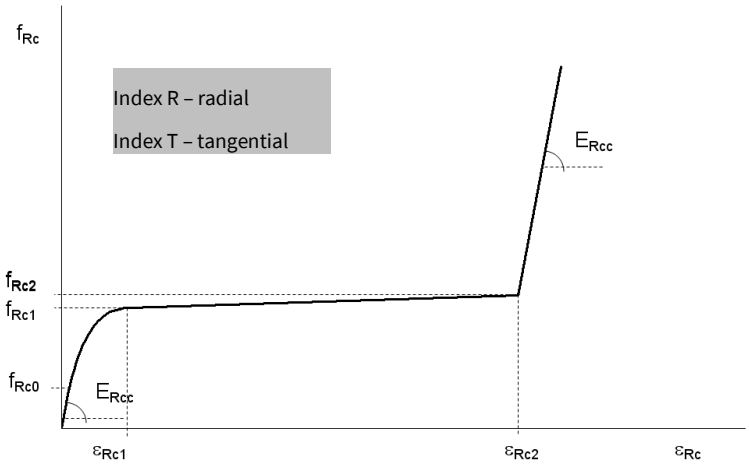

Fig. 2-11: Wood model – uniaxial stress-strain curve in radial or tangential compression (perpendicular to fiber direction)

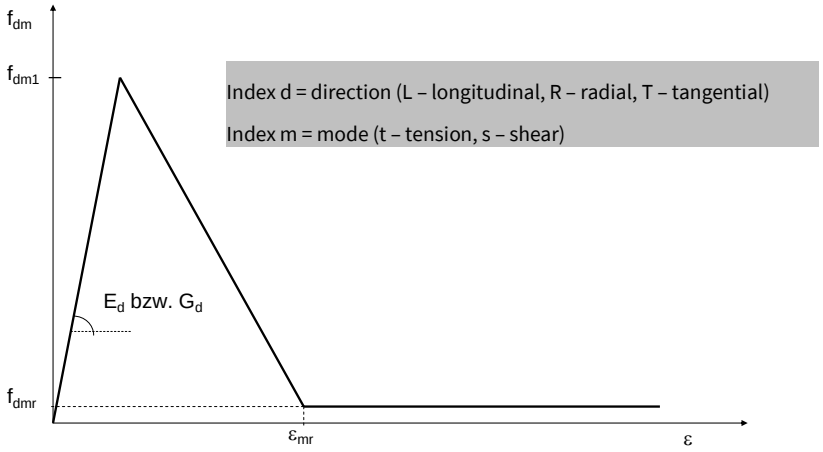

Fig. 2-12: Wood model – uniaxial stress-strain curve for shear failure and tensile failure

2.4.1. Base material parameters

The law 33 supports different types of hardening/softening functions for the tensile failure and the shear failure. The hardening/softening behavior in compression is identical in all models. The specific type of softening is defined by parameter *mlaw*. Only some material parameters depend on the softening law. Table 2.11 summarizes all those parameters which are identical

in all mlaw's. Additionally, the wood model can be coupled with the anisotropic Mohr-Coulomb model with tension cut-off.

Table 2.11: Wood model – base parameters

	1	2	3	4	5	6	7	8	9	10
1-10	**33**	f_{Lt}	f_{Lc}	f_{Rt}	f_{Rc}	f_{Tt}	f_{Tc}	f_{RLs}	f_{RTs}	ntf
11-20	ϕ	c	ψ	ϕ^*	c^*	f_t	α	β	f_t^*	
21-30	Ω_{Lc0}	κ_{Lc1}	Ω_{Lc2}	κ_{Lc2}	κ_{Lc3}				f_{TLs}	f_{TRs}
31-40	Ω_{Rc0}	κ_{Rc1}	Ω_{Rc2}	κ_{Rc2}		Ω_{Tc0}	κ_{Tc1}	Ω_{Tc2}	κ_{Tc2}	mlaw
41-50	Ω_{Ltr}		Ω_{Rtr}		Ω_{Ttr}		Ω_{RLsr}		Ω_{RTsr}	
51-60	Ω_{TLsr}		Ω_{TRsr}						direc	wr
61-70	Elem	Intpt	eps	geps	maxit	cutmax			algo	ktuser
71-80										

Wood parameters:

- initial strength

parameter	description	SI unit	range
f_{Lt}	uniaxial tensile strength in longitudinal direction (in fiber direction)	[N/m^2]	$f_{Lt} > 0$
f_{Lc}	uniaxial compressive strength in longitudinal direction (in fibre direction)	[N/m^2]	$f_{Lc} > 0$
f_{Rt}	uniaxial tensile strength in radial direction	[N/m^2]	$f_{Rt} > 0$
f_{Rc}	uniaxial compressive strength in radial direction	[N/m^2]	$f_{Rc} > 0$
f_{Tt}	uniaxial tensile strength in tangential direction	[N/m^2]	$f_{Tt} > 0$
f_{Tc}	uniaxial compressive strength in tangential direction	[N/m^2]	$f_{Tc} > 0$
f_{RLs}	radial/longitudinal shear strength	[N/m^2]	$f_{RLs} > 0$
f_{RTs}	radial/tangential shear strength	[N/m^2]	$f_{RTs} > 0$
f_{TLs}	tangential/longitudinal shear strength	[N/m^2]	$f_{TLs} > 0$
f_{TRs}	tangential/radial shear strength	[N/m^2]	$f_{TRs} > 0$

- hardening/softening parameters longitudinal compression, cf. Fig. 2-10

parameter	description	SI unit	range
Ω_{Lc0}	relative stress level at start of initial hardening	[-]	$0 < \Omega_{Lc0} < 1$
κ_{Lc1}	hardening variable (plastic strain) at longitudinal compressive strength	[-]	$\kappa_{Lc1} > 0$
Ω_{Lc2}	relative stress level in ideal plastic domain	[-]	$\Omega_{Lc2} > 0$
κ_{Lc2}	hardening variable (plastic strain) defining start of ideal plastic domain	[-]	$\kappa_{Lc2} > \kappa_{Lc1}$
κ_{Lc3}	hardening variable (plastic strain) defining end of ideal plastic domain	[-]	$\kappa_{Lc3} > \kappa_{Lc2}$

- hardening/softening parameters radial compression, cf. Fig. 2-11

parameter	description	SI unit	range
Ω_{Rc0}	relative stress level at start of initial hardening	[-]	$0 < \Omega_{Rc0} < 1$
κ_{Rc1}	hardening variable (plastic strain) at radial compressive strength	[-]	$\kappa_{Rc1} > 0$
Ω_{Rc2}	relative stress level at end of plastic domain	[-]	$\Omega_{Rc2} > 0$
κ_{Rc2}	hardening variable (plastic strain) defining end of plastic domain	[-]	$\kappa_{Rc2} > \kappa_{Rc1}$

- hardening/softening parameters tangential compression, cf. Fig. 2-11

parameter	description	SI unit	range
Ω_{Tc0}	relative stress level at start of initial hardening	[-]	$0 < \Omega_{Tc0} < 1$
κ_{Tc1}	hardening variable (plastic strain) at tangential compressive strength	[-]	$\kappa_{Tc1} > 0$

parameter	description	SI unit	range
Ω_{Tc2}	relative stress level at end of plastic domain	[-]	$\Omega_{Tc2} > 0$
κ_{Tc2}	hardening variable (plastic strain) defining end of plastic domain	[-]	$\kappa_{Tc2} > \kappa_{Tc1}$

- shear/tensile strength softening parameters

parameter	description	SI unit	range
Ω_{Ltr}	relative residual longitudinal tensile strength	[-]	$\Omega_{Ltr} > 0$
Ω_{Rtr}	relative residual radial tensile strength	[-]	$\Omega_{Rtr} > 0$
Ω_{Ttr}	relative residual tangential tensile strength	[-]	$\Omega_{Ttr} > 0$
Ω_{RLsr}	relative residual radial/longitudinal shear strength	[-]	$\Omega_{RLsr} > 0$
Ω_{RTsr}	relative residual radial/tangential shear strength	[-]	$\Omega_{RTsr} > 0$
Ω_{TLsr}	relative residual tangential/longitudinal shear strength	[-]	$\Omega_{TLsr} > 0$
Ω_{TRsr}	relative residual tangential/radial shear strength	[-]	$\Omega_{TRsr} > 0$
mlaw	softening law switch 0 – linear softening 1 – fracture energy based exponential softening	[-]	0 or 1

Joint parameters:

parameter	description	SI unit	range
ntf	number of joint sets	[-]	0 or 1
c	joint cohesion	[N/m²]	c > 0
c*	residual joint cohesion	[N/m²]	$0 < c^* \leq c$
ϕ	joint friction angle	[°]	$0° < \phi < 90°$
ϕ^*	residual joint friction angle	[°]	$0° < \phi^* \leq \phi$
ψ	joint dilatancy angle	[°]	$0° < \psi \leq \phi$
f_t	joint tensile strength	[N/m²]	$f_t > 0$
f_t^*	residual joint tensile strength	[N/m²]	$0 < f_t^* \leq f_t$
α	negative rotation about element Z-axis	[°]	
β	positive rotation about new Y-axis	[°]	

Control parameters:

parameter	description	SI unit	range
direc	orientation of the joints relative to the element coordinate system, cf. Table 2.12	[-]	0, 1, 2

Table 2.12: Wood model – definition of control parameter direc.

stress component	direc=0 (R,T,L)	direc=1 (L,R,T)	direc=2 (L,T,R)	direc=3 (T,L,R)
σ_{xx}	σ_{RR}	σ_{LL}	σ_{LL}	σ_{TT}
σ_{yy}	σ_{TT}	σ_{RR}	σ_{TT}	σ_{LL}
σ_{zz}	σ_{LL}	σ_{TT}	σ_{RR}	σ_{RR}
σ_{xy}	σ_{RT}	σ_{LR}	σ_{LT}	σ_{LT}
σ_{yz}	σ_{LT}	σ_{RT}	σ_{TR}	σ_{LR}
σ_{xz}	σ_{RL}	σ_{LT}	σ_{LR}	σ_{TR}

2.4.2. Additional material parameters for linear softening (mlaw 0)

In the law 33, mlaw 0 linear softening functions are applied in tensile and shear failure, cf. Fig. 2-12. The corresponding material parameters are summarized in Table 2.13.

Table 2.13: Wood model with linear softening – parameters

	1	2	3	4	5	6	7	8	9	10
1-10	**33**	f_{Lt}	f_{Lc}	f_{Rt}	f_{Rc}	f_{Tt}	f_{Tc}	f_{RLs}	f_{RTs}	ntf
11-20	ϕ	c	Ψ	ϕ^*	c^*	f_t	α	β	f_t^*	
21-30	Ω_{Lc0}	κ_{Lc1}	Ω_{Lc2}	κ_{Lc2}	κ_{Lc3}				f_{TLs}	f_{TRs}
31-40	Ω_{Rc0}	κ_{Rc1}	Ω_{Rc2}	κ_{Rc2}		Ω_{Tc0}	κ_{Tc1}	Ω_{Tc2}	κ_{Tc2}	**0**
41-50	Ω_{Ltr}	$\boldsymbol{\kappa_{Ltr}}$	Ω_{Rtr}	$\boldsymbol{\kappa_{Rtr}}$	Ω_{Ttr}	$\boldsymbol{\kappa_{Ttr}}$	Ω_{RLsr}	$\boldsymbol{\kappa_{RLsr}}$	Ω_{RTsr}	$\boldsymbol{\kappa_{RTsr}}$
51-60	Ω_{TLsr}	$\boldsymbol{\kappa_{TLsr}}$	Ω_{TRsr}	$\boldsymbol{\kappa_{TRsr}}$					direc	wr
61-70	Elem	Intpt	eps	geps	maxit	cutmax			algo	ktuser
71-80										

- additional shear/tensile strength softening parameters

parameter	description	SI unit	range
κ_{Ltr}	limit plastic strain for longitudinal tension	[-]	$\kappa_{Ltr} > 0$
κ_{Rtr}	limit plastic strain for radial tension	[-]	$\kappa_{Rtr} > 0$
κ_{Ttr}	limit plastic strain for tangential tension	[-]	$\kappa_{Ttr} > 0$
κ_{RLsr}	limit plastic strain for radial/longitudinal shear	[-]	$\kappa_{RLsr} > 0$
κ_{RTsr}	limit plastic strain for radial/tangential shear	[-]	$\kappa_{RTsr} > 0$
κ_{TLsr}	limit plastic strain for tangential/longitudinal shear	[-]	$\kappa_{TLsr} > 0$
κ_{TRsr}	limit plastic strain for tangential/radial shear	[-]	$\kappa_{TRsr} > 0$

2.4.3. Additional material parameters for exponential softening (mlaw 1)

In law the 33, mlaw 1, fracture energy based exponential softening functions are applied in tensile and shear failure. The area specific fracture energy is regularized with respect to the element size. The corresponding material parameters are summarized in Table 2.14.

Table 2.14: Wood model with exponential softening – parameters

	1	2	3	4	5	6	7	8	9	10
1-10	**33**	f_{Lt}	f_{Lc}	f_{Rt}	f_{Rc}	f_{Tt}	f_{Tc}	f_{RLs}	f_{RTs}	ntf
11-20	ϕ	c	Ψ	ϕ^*	c^*	f_t	α	β	f_t^*	
21-30	Ω_{Lc0}	κ_{Lc1}	Ω_{Lc2}	κ_{Lc2}	κ_{Lc3}				f_{TLs}	f_{TRs}
31-40	Ω_{Rc0}	κ_{Rc1}	Ω_{Rc2}	κ_{Rc2}		Ω_{Tc0}	κ_{Tc1}	Ω_{Tc2}	κ_{Tc2}	**1**
41-50	Ω_{Ltr}	$\boldsymbol{G^I_{fL}}$	Ω_{Rtr}	$\boldsymbol{G^I_{fR}}$	Ω_{Ttr}	$\boldsymbol{G^I_{fT}}$	Ω_{RLsr}	$\boldsymbol{G^{II}_{fRL}}$	Ω_{RTsr}	$\boldsymbol{G^{II}_{fRT}}$
51-60	Ω_{TLsr}	$\boldsymbol{G^{II}_{fTL}}$	Ω_{TRsr}	$\boldsymbol{G^{II}_{fTR}}$					direc	wr
61-70	Elem	Intpt	eps	geps	maxit	cutmax			algo	ktuser
71-80										

- additional shear/tensile strength softening parameters

parameter	description	SI unit	range
G^I_{fL}	area specific mode-I fracture energy for longitudinal tensile failure	[Nm/m^2]	$G^I_{fL} > 0$
G^I_{fR}	area specific mode-I fracture energy for radial tensile failure	[Nm/m^2]	$G^I_{fR} > 0$
G^I_{fT}	area specific mode-I fracture energy for tangential tensile failure	[Nm/m^2]	$G^I_{fT} > 0$
G^{II}_{fRL}	area specific mode-II fracture energy for radial/longitudinal shear failure	[Nm/m^2]	$G^{II}_{fRL} > 0$
G^{II}_{fRT}	area specific mode-II fracture energy for radial/tangential shear failure	[Nm/m^2]	$G^{II}_{fRT} > 0$
G^{II}_{fTL}	area specific mode-II fracture energy for tangential/longitudinal shear failure	[Nm/m^2]	$G^{II}_{fTL} > 0$
G^{II}_{fTR}	area specific mode-II fracture energy for tangential/radial shear failure	[Nm/m^2]	$G^{II}_{fTR} > 0$

2.4.4. State variables

In this model **10** state variables are defined, cf. Table 2.15.

Table 2.15: Wood model – state variables

state variable	description
1	number representing the activity of individual yield surfaces (failure modes)
2	hardening variable for longitudinal tensile failure
3	hardening variable for longitudinal compressive failure
4	hardening variable representing evolution of cracks parallel to LT-plane
5	hardening variable for radial compressive failure
6	hardening variable representing evolution of cracks parallel to RL-plane
7	hardening variable for tangential compressive failure
8	accumulated tangential plastic strains due to Mohr-Coulomb failure of joint
9	accumulated normal plastic strains due to Mohr-Coulomb failure of joint
10	accumulated normal plastic strains due to tensile failure of joint

2.4.5. Activity encoding

The activity of the individual yield surfaces is encoded into a single number. The following table shows the encoding if a single yield surface fails. If multiple yield surfaces fail, then the corresponding numbers are added.

number	activity
1	longitudinal tensile failure (fiber rupture)
10	longitudinal compressive failure (fiber compression)
100	evolution of cracks parallel to LT-plane
1 000	radial compressive failure
10 000	evolution of cracks parallel to LR-plane
100 000	tangential compressive failure
1 000 000	shear failure of joint (Mohr-Coulomb yield surface)
10 000 000	tensile failure of joint (tension cut-off yield surface)

2.5. Orthotropic Boxed Value Model for Additive Manufacturing

The material model for additive manufacturing is based on the orthotropic boxed value concept introduced in section 2.4. In contrast to the wood model, the evolution of the strength parameters can be defined as multi-linear functions. Furthermore, the model can be combined with an implicit creep law.

2.5.1. Material parameters

The material parameters of law 34 are summarized in Table 2.16**.**

Table 2.16: Orthotropic boxed value model for additive manufacturing – base parameters

	1	2	3	4	5	6	7	8	9	10
1-10	**34**	f_{Lt}	f_{Lc}	f_{Rt}	f_{Rc}	f_{Tt}	f_{Tc}	f_{RLs}	f_{RTs}	
11-20										
21-30									f_{TLs}	f_{TRs}
31-40	claw	c_1	c_2	c_3	c_4	c_5	c_6	c_7	c_8	c_9
41-50	c_{10}	c_{11}	c_{12}	c_{13}	c_{14}	c_{15}	c_{16}	c_{17}	c_{18}	T_{offset}
51-60									direc	wr
61-70	Elem	Intpt	eps	geps	maxit	cutmax			algo	ktuser
71-80										

Material parameters

- initial strength parameters of orthotropic boxed value model

parameter	description	SI unit	range
f_{Lt}	uniaxial tensile strength in longitudinal direction	[N/m²]	$f_{Lt} > 0$
f_{Lc}	uniaxial compressive strength in longitudinal direction	[N/m²]	$f_{Lc} > 0$
f_{Rt}	uniaxial tensile strength in radial direction	[N/m²]	$f_{Rt} > 0$
f_{Rc}	uniaxial compressive strength in radial direction	[N/m²]	$f_{Rc} > 0$
f_{Tt}	uniaxial tensile strength in tangential direction	[N/m²]	$f_{Tt} > 0$
f_{Tc}	uniaxial compressive strength in tangential direction	[N/m²]	$f_{Tc} > 0$
f_{RLs}	radial/longitudinal shear strength	[N/m²]	$f_{RLs} > 0$
f_{RTs}	radial/tangential shear strength	[N/m²]	$f_{RTs} > 0$
f_{TLs}	tangential/longitudinal shear strength	[N/m²]	$f_{TLs} > 0$
f_{TRs}	tangential/radial shear strength	[N/m²]	$f_{TRs} > 0$

- control parameters

parameter	description	SI unit	range
direc	definition of the material axes with respect to the element coordinate system, cf. Table 2.12 direc=0: x=R, y=T, z=L direc=1: x=L, y=R, z=T direc=2: x=L, y=T, z=R direc=3: x=T, y=L, z=R	[-]	0, 1, 2, 3

Note: The direc flag applies only to the plasticity part of the model (anisotropic strength definition). The elastic parameters, Young's moduli, Poisson's ratio and shear moduli, are defined in any case in the element coordinate system.

Creep parameters:

The creep parameters are explained in Section 2.8.

2.5.2. State variables

In this model **14** state variables are defined, cf. Table 2.17. If creep is disabled, the the number of state variables can be reduced to **7**.

Table 2.17: Orthotropic boxed value model for additive manufacturing – state variables

state variable	description
1	number representing the activity of individual yield surfaces (failure modes)
2	hardening variable for longitudinal tensile failure
3	hardening variable for longitudinal compressive failure
4	hardening variable representing evolution of cracks parallel to LT-plane
5	hardening variable for radial compressive failure
6	hardening variable representing evolution of cracks parallel to RL-plane
7	hardening variable for tangential compressive failure
8	Creep strain in x direction
9	Creep strain in y direction
10	Creep strain in z direction
11	Creep strain in xy direction
12	Creep strain in yz direction
13	Creep strain in xz direction
14	Accumulated creep strain $\int_0^t \dot{\varepsilon_{cr}} dt$

2.5.3. Activity encoding

The activity of the individual yield surfaces is encoded into a single number. The following table shows the encoding if a single yield surface fails. If multiple yield surfaces fail, then the corresponding numbers are added.

number	activity
1	longitudinal tensile failure
10	longitudinal compressive failure
100	evolution of cracks parallel to LT-plane
1 000	radial compressive failure
10 000	evolution of cracks parallel to LR-plane
100 000	tangential compressive failure

2.5.4. Optional multi-linear hardening softening

In addition, multi-linear hardening/softening functions with up to 10 support points (Fig. 2-13**)** can be defined for each of the strength parameters separately. The corresponding stress strain curve parameters are summarized in Table 2.18. The number of points on the stress-strain curve is automatically detected based on kappa. The stress strain curve definition stops, if kappa does not further increase, e.g. is zero.

Note: The size of the TBDATA field must be 280, even if stress-strain curves are not defined for all strength parameters.

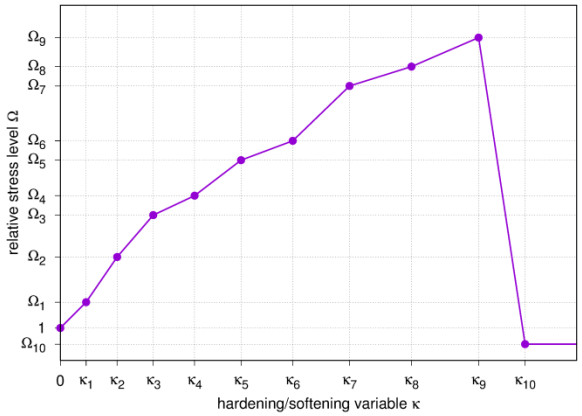

Fig. 2-13: Orthotropic boxed value model for additive manufacturing – multilinear-hardening softening function

Table 2.18: Orthotropic boxed value model for additive manufacturing – optional stress-strain curve parameters

	1	2	3	4	5	6	7	8	9	10
81-90	K_{Lt1}	K_{Lt2}	K_{Lt3}	K_{Lt4}	K_{Lt5}	K_{Lt6}	K_{Lt7}	K_{Lt8}	K_{Lt9}	K_{Lt10}
91-100	Ω_{Lt1}	Ω_{Lt2}	Ω_{Lt3}	Ω_{Lt4}	Ω_{Lt5}	Ω_{Lt6}	Ω_{Lt7}	Ω_{Lt8}	Ω_{Lt9}	Ω_{Lt10}
101-110	K_{Lc1}	K_{Lc2}	K_{Lc3}	K_{Lc4}	K_{Lc5}	K_{Lc6}	K_{Lc7}	K_{Lc8}	K_{Lc9}	K_{Lc10}
111-120	Ω_{Lc1}	Ω_{Lc2}	Ω_{Lc3}	Ω_{Lc4}	Ω_{Lc5}	Ω_{Lc6}	Ω_{Lc7}	Ω_{Lc8}	Ω_{Lc9}	Ω_{Lc10}
121-130	K_{Rt1}	K_{Rt2}	K_{Rt3}	K_{Rt4}	K_{Rt5}	K_{Rt6}	K_{Rt7}	K_{Rt8}	K_{Rt9}	K_{Rt10}
131-140	Ω_{Rt1}	Ω_{Rt2}	Ω_{Rt3}	Ω_{Rt4}	Ω_{Rt5}	Ω_{Rt6}	Ω_{Rt7}	Ω_{Rt8}	Ω_{Rt9}	Ω_{Rt10}
141-150	K_{Rc1}	K_{Rc2}	K_{Rc3}	K_{Rc4}	K_{Rc5}	K_{Rc6}	K_{Rc7}	K_{Rc8}	K_{Rc9}	K_{Rc10}
151-160	Ω_{Rc1}	Ω_{Rc2}	Ω_{Rc3}	Ω_{Rc4}	Ω_{Rc5}	Ω_{Rc6}	Ω_{Rc7}	Ω_{Rc8}	Ω_{Rc9}	Ω_{Rc10}
161-170	K_{Tt1}	K_{Tt2}	K_{Tt3}	K_{Tt4}	K_{Tt5}	K_{Tt6}	K_{Tt7}	K_{Tt8}	K_{Tt9}	K_{Tt10}
171-180	Ω_{Tt1}	Ω_{Tt2}	Ω_{Tt3}	Ω_{Tt4}	Ω_{Tt5}	Ω_{Tt6}	Ω_{Tt7}	Ω_{Tt8}	Ω_{Tt9}	Ω_{Tt10}
181-190	K_{Tc1}	K_{Tc2}	K_{Tc3}	K_{Tc4}	K_{Tc5}	K_{Tc6}	K_{Tc7}	K_{Tc8}	K_{Tc9}	K_{Tc10}
191-200	Ω_{Tc1}	Ω_{Tc2}	Ω_{Tc3}	Ω_{Tc4}	Ω_{Tc5}	Ω_{Tc6}	Ω_{Tc7}	Ω_{Tc8}	Ω_{Tc9}	Ω_{Tc10}
201-210	K_{RLs1}	K_{RLs2}	K_{RLs3}	K_{RLs4}	K_{RLs5}	K_{RLs6}	K_{RLs7}	K_{RLs8}	K_{RLs9}	K_{RLs10}
211-220	Ω_{RLs1}	Ω_{RLs2}	Ω_{RLs3}	Ω_{RLs4}	Ω_{RLs5}	Ω_{RLs6}	Ω_{RLs7}	Ω_{RLs8}	Ω_{RLs9}	Ω_{RLs10}
221-230	K_{RTs1}	K_{RTs2}	K_{RTs3}	K_{RTs4}	K_{RTs5}	K_{RTs6}	K_{RTs7}	K_{RTs8}	K_{RTs9}	K_{RTs10}
231-240	Ω_{RTs1}	Ω_{RTs2}	Ω_{RTs3}	Ω_{RTs4}	Ω_{RTs5}	Ω_{RTs6}	Ω_{RTs7}	Ω_{RTs8}	Ω_{RTs9}	Ω_{RTs10}
241-250	K_{TLs1}	K_{TLs2}	K_{TLs3}	K_{TLs4}	K_{TLs5}	K_{TLs6}	K_{TLs7}	K_{TLs8}	K_{TLs9}	K_{TLs10}
251-260	Ω_{TLs1}	Ω_{TLs2}	Ω_{TLs3}	Ω_{TLs4}	Ω_{TLs5}	Ω_{TLs6}	Ω_{TLs7}	Ω_{TLs8}	Ω_{TLs9}	Ω_{TLs10}
261-270	K_{TRs1}	K_{TRs2}	K_{TRs3}	K_{TRs4}	K_{TRs5}	K_{TRs6}	K_{TRs7}	K_{TRs8}	K_{TRs9}	K_{TRs10}
271-280	Ω_{TRs1}	Ω_{TRs2}	Ω_{TRs3}	Ω_{TRs4}	Ω_{TRs5}	Ω_{TRs6}	Ω_{TRs7}	Ω_{TRs8}	Ω_{TRs9}	Ω_{TRs10}

2.6. Cable/Winding material model

The cable material model is based on the orthotropic boxed value concept, introduced in section section 2.4. In general, the orthotropic boxed value model describes strength anisotropies in the longitudinal, radial, and tangential directions. Furthermore, different strength definitions in tension and compression can be considered.

Since the material exhibits transversely isotropic behavior, the strength definitions can be simplified. Assuming isotropy in the RT-plane (radial-tangential) the simplified yield functions can be written as:

- tensile failure in longitudinal direction (in wire direction)

$$F_1 = \sigma_{LL} - f_{Lt}\Omega_{Lt} = 0 \tag{2.7}$$

- compressive failure in longitudinal direction (in wire direction)

$$F_2 = -\sigma_{LL} - f_{Lc}\Omega_{Lc} = 0 \tag{2.8}$$

- initiation and the evolution of cracks parallel to the LT-plane

$$F_3 = \left(\frac{\langle\sigma_{RR}\rangle}{f_{Tt}\Omega_{Tt}}\right)^2 + \left(\frac{\sigma_{RL}}{f_{TLs}\Omega_{TLs}}\right)^2 + \left(\frac{\sigma_{RT}}{f_{TRs}\Omega_{TRs}}\right)^2 - 1 = 0 \tag{2.9}$$

  with

$$\langle\sigma_{RR}\rangle = \begin{cases} 0 & \sigma_{RR} \leq 0 \\ \sigma_{RR} & \sigma_{RR} > 0 \end{cases}$$

- radial compressive failure (perpendicular to the wire)

$$F_4 = -\sigma_{RR} - f_{Tc}\Omega_{Tc} = 0 \tag{2.10}$$

- initiation and the evolution of cracks parallel to the LR-plane

$$F_5 = \frac{\sigma_{TT}}{f_{Tt}\Omega_{Tt}} + \left(\frac{\sigma_{TR}}{f_{TRs}\Omega_{TRs}}\right)^2 + \left(\frac{\sigma_{TL}}{f_{TLs}\Omega_{TLs}}\right)^2 - 1 = 0, \tag{2.11}$$

- compressive failure in tangential direction (perpendicular to the wire)

$$F_6 = -\sigma_{TT} - f_{Tc}\Omega_{Tc} = 0. \tag{2.12}$$

In the above equations f are the initial strength values and the Ω functions describe the evolution of the corresponding strength, cf. Fig. 2-14, Fig. 2-15 and Fig. 2-16. Capital subscripts correspond to the directions longitudinal (L), radial (R), or tangential (T). Lower case subscripts relate to compression (c), tension (t), or shear (s).

Note: Although the material parameters exhibit transverse isotropy, the definition of the yield surfaces is still orthotropic.

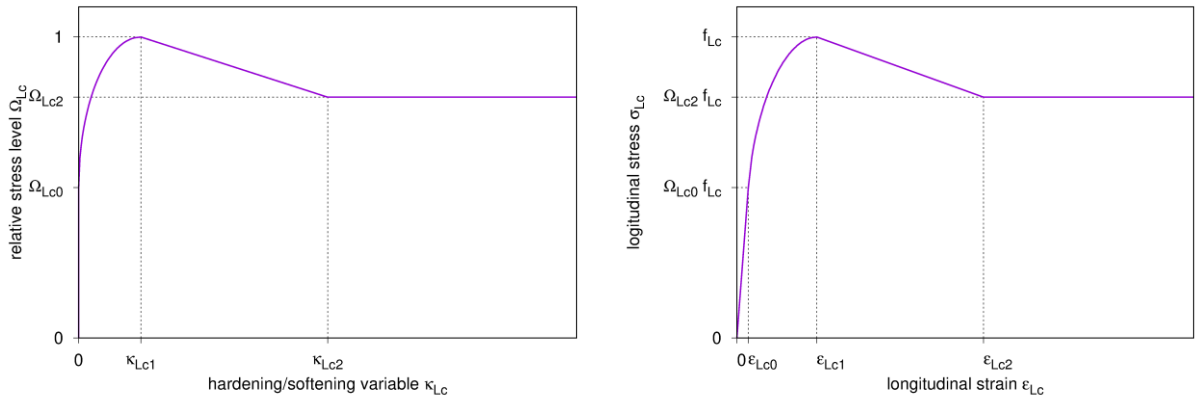

Fig. 2-14: Cable model – longitudinal compression – hardening/softening law (left) and uniaxial stress-strain relationship (right)

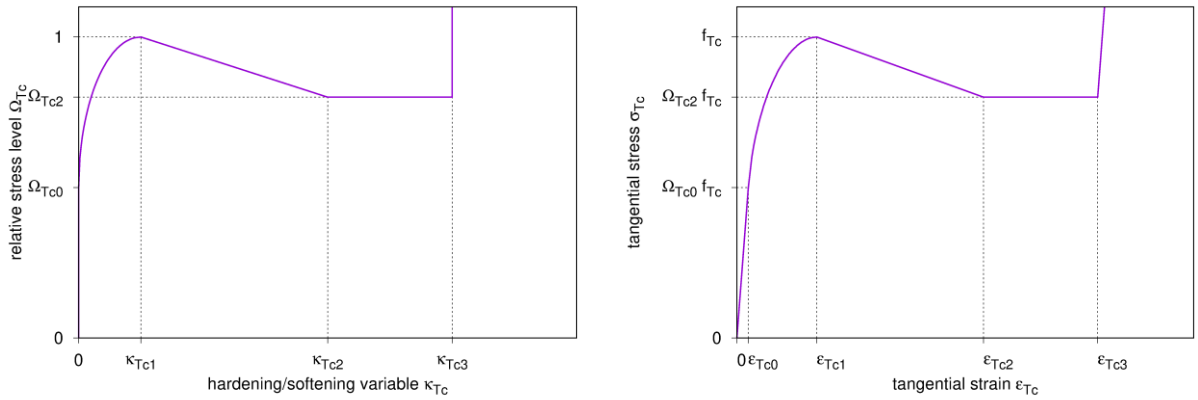

Fig. 2-15: Cable model – tangential compression – hardening/softening law (left) and uniaxial stress-strain relationship (right)

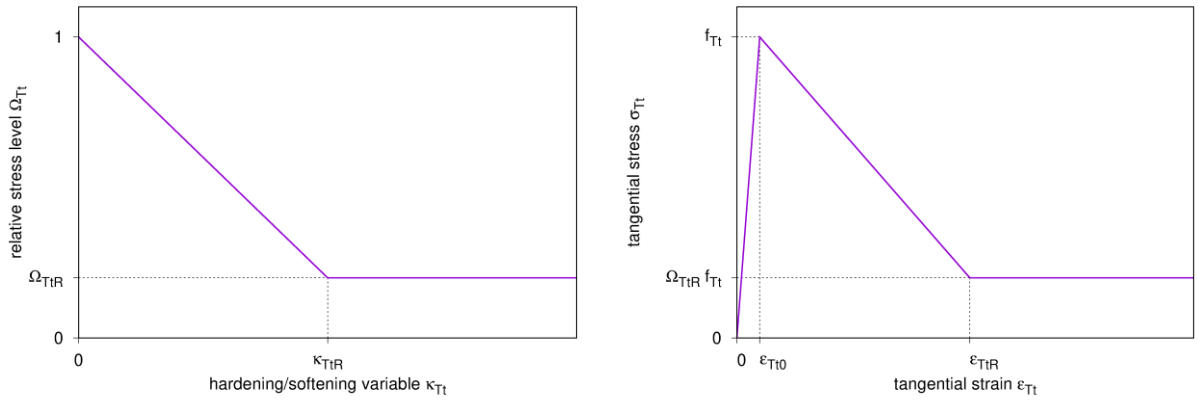

Fig. 2-16: Cable model – shear and tension – hardening/softening law (left) and uniaxial stress-strain relationship (right)

Note: Fig. 2-16 shows the hardening/softening law and the resulting uniaxial stress-strain relationship for tangential tension. The same model applies to longitudinal tension, out-of-plane shear, and in-plane shear.

2.6.1. Material parameters

The parameters of law 141 are summarized in Table 2.19.

Table 2.19: Cable model – parameters

	1	2	3	4	5	6	7	8	9	10
1-10	**141**	f_{Lt}	f_{Lc}			f_{Tt}	f_{Tc}			
11-20										
21-30	Ω_{Lc0}	κ_{Lc1}	Ω_{Lc2}	κ_{Lc2}			κ_{Tc3}		f_{TLs}	f_{TRs}
31-40						Ω_{Tc0}	κ_{Tc1}	Ω_{Tc2}	κ_{Tc2}	
41-50	Ω_{Ltr}	κ_{Ltr}			Ω_{Ttr}	κ_{Ttr}				
51-60	Ω_{TLsr}	κ_{TLsr}	Ω_{TRsr}	κ_{TRsr}					direc	wr
61-70	Elem	Intpt	eps	geps	maxit	cutmax			algo	ktuser
71-80										

Initial strength parameters

parameter	description	SI unit	range
f_{Lt}	uniaxial tensile strength in longitudinal direction (in wire direction)	[N/m^2]	$f_{Lt} > 0$
f_{Lc}	uniaxial compressive strength in longitudinal direction (in wire direction)	[N/m^2]	$f_{Lc} > 0$
f_{Tt}	uniaxial tensile strength in RT-plane (perpendicular to the wire)	[N/m^2]	$f_{Tt} > 0$
f_{Tc}	uniaxial compressive strength in RT-plane (perpendicular to the wire)	[N/m^2]	$f_{Tc} > 0$
f_{TLs}	out-of-plane shear strength	[N/m^2]	$f_{TLs} > 0$
f_{TRs}	in-plane (RT) shear strength	[N/m^2]	$f_{TRs} > 0$

Hardening/softening parameters

- longitudinal compression (wire direction), cf. Fig. 2-14

parameter	Description	SI unit	range
Ω_{Lc0}	relative stress level at start of initial hardening	[-]	$0 < \Omega_{Lc0} < 1$
κ_{Lc1}	hardening variable (plastic strain) at longitudinal compressive strength	[-]	$\kappa_{Lc1} > 0$
Ω_{Lc2}	relative stress level in ideal plastic domain	[-]	$\Omega_{Lc2} > 0$
κ_{Lc2}	hardening variable (plastic strain) defining start of ideal plastic domain	[-]	$\kappa_{Lc2} > \kappa_{Lc1}$

- RT-plane compression (perpendicular to the wire), cf. Fig. 2-15

parameter	Description	SI unit	range
Ω_{Tc0}	relative stress level at start of initial hardening	[-]	$0 < \Omega_{Tc0} < 1$
κ_{Tc1}	hardening variable (plastic strain) at tangential compressive strength	[-]	$\kappa_{Tc1} > 0$
Ω_{Tc2}	relative stress level at end of plastic domain	[-]	$\Omega_{Tc2} > 0$
κ_{Tc2}	hardening variable (plastic strain) defining end of plastic domain	[-]	$\kappa_{Tc2} > \kappa_{Tc1}$
κ_{Tc3}	hardening variable (plastic strain) defining end of ideal plastic domain	[-]	$\kappa_{Tc3} > \kappa_{Tc2}$

- shear/tensile strength softening parameters, cf. Fig. 2-16

parameter	description	SI unit	range
Ω_{Ltr}	relative residual longitudinal tensile strength	[-]	$\Omega_{Ltr} > 0$
Ω_{Ttr}	relative residual RT-plane tensile strength	[-]	$\Omega_{Ttr} > 0$
Ω_{TLsr}	relative residual out-of-plane shear strength	[-]	$\Omega_{TLsr} > 0$
Ω_{TRsr}	relative residual in-plane shear strength	[-]	$\Omega_{TRsr} > 0$
κ_{Ltr}	limit plastic strain for longitudinal tension	[-]	$\kappa_{Ltr} > 0$
κ_{Ttr}	limit plastic strain for RT-plane tension	[-]	$\kappa_{Ttr} > 0$

parameter	description	SI unit	range
κ_{TLsr}	limit plastic strain for out-of-plane shear	[-]	$\kappa_{TLsr} > 0$
κ_{TRsr}	limit plastic strain for in-plane shear	[-]	$\kappa_{TRsr} > 0$

control parameters

parameter	description	SI unit	range
direc	orientation of material axes relative to the element coordinate system, cf. Table 2.20	[-]	0, 1, 2, 3

Table 2.20: Cable model – definition of control parameter direc.

stress component	direc=0 (R,T,L)	direc=1 (L,R,T)	direc=2 (L,T,R)	direc=3 (T,L,R)
σ_{xx}	σ_{RR}	σ_{LL}	σ_{LL}	σ_{TT}
σ_{yy}	σ_{TT}	σ_{RR}	σ_{TT}	σ_{LL}
σ_{zz}	σ_{LL}	σ_{TT}	σ_{RR}	σ_{RR}
σ_{xy}	σ_{RT}	σ_{LR}	σ_{LT}	σ_{LT}
σ_{yz}	σ_{LT}	σ_{RT}	σ_{TR}	σ_{LR}
σ_{xz}	σ_{RL}	σ_{LT}	σ_{LR}	σ_{TR}

2.6.2. State variables

In this model **10** state variables are defined, cf.Table 2.21.

Table 2.21: Cable model – state variables

state variable	description
1	number representing the activity of individual yield surfaces (failure modes)
2	hardening variable for longitudinal tensile failure
3	hardening variable for longitudinal compressive failure
4	hardening variable representing evolution of cracks parallel to LT-plane
5	hardening variable for radial compressive failure
6	hardening variable representing evolution of cracks parallel to RL-plane
7	hardening variable for tangential compressive failure
8…10	currently not used

2.6.3. Activity encoding

The activity of the individual yield surfaces is encoded into a single number. The following table shows the encoding if a single yield surface fails. If multiple yield surfaces fail, then the corresponding numbers are added.

number	activity
1	longitudinal tensile failure
10	longitudinal compressive failure
100	evolution of cracks parallel to LT-plane
1 000	radial compressive failure
10 000	evolution of cracks parallel to LR-plane
100 000	tangential compressive failure

2.7. Laminated sheet package

Successful electric drive concepts are based on efficient electric motor designs. Typically, part of the core of an electric motor is fabricated using stacked laminated sheets. The stacked package is exposed to a multitude of different loading conditions during initial production and later use in the vehicle. The material behavior is inherently non-linear, encompassing shear failure, buckling (fan out) as well as metal yielding including softening and hardening effects. The laminated sheet package material model consists of several distinct yield surfaces that describe these specific failure modes.

The base material, which consists of stacked, isolated metal sheets exhibits anisotropic failure modes. An illustration of the stacked sheets is provided in Fig. 2-17**.** The in-plane direction $\vec{p}$ is defined by the local element coordinate system directions x and y. The orthogonal axis is defined by the local z-direction.

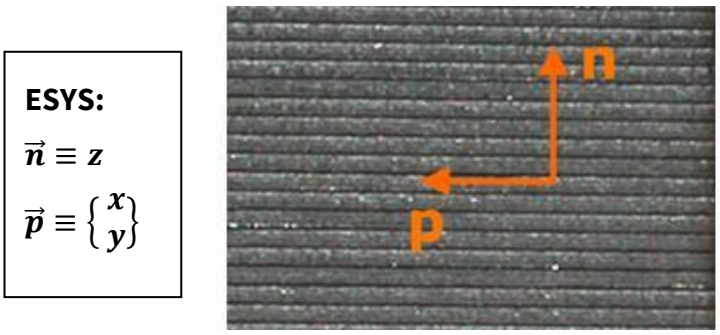

Fig. 2-17: Laminated sheet package with local coordinate system

The fully associative yield behavior of the anisotropic base material, i.e. the metal sheets is defined by a von Mises J2 plasticity yield curve

$$F_1 = \sqrt{3J_2} - \Omega(\kappa)\sigma_v = 0. \tag{2.13}$$

Here, J_2 is the second deviatoric stress invariant, $\Omega(\kappa)$ defines a multi-linear hardening/softening curve with up to 10 distinct plastic strain/relative stress data points (see Fig. 2-18) and σ_v is the initial yield strength.

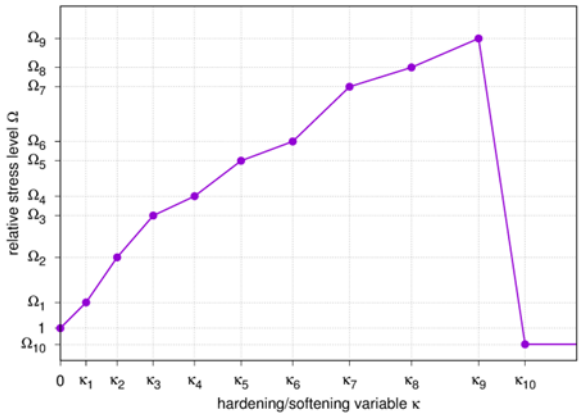

Fig. 2-18: Laminated sheet package – multi-linear hardening and softening function for von Mises yield criterion

The sheet buckling due to excessive compressive stresses in the transverse direction is modelled using two separate buckling strength yield surfaces. The buckling strength in the local x-direction is specified as

$$F_2 = \sigma_{zz} - \frac{\mathrm{f_{tb}}}{\eta_x \sigma_v}\sigma_{xx} - f_{tb} = 0, \tag{2.14}$$

whereas the buckling strength in local y-direction is given as

$$F_3 = \sigma_{zz} - \frac{\mathrm{f_{tb}}}{\eta_y \sigma_v}\sigma_{yy} - f_{tb} = 0. \tag{2.15}$$

The buckling strength yield criteria depend on the compressive in-plane stresses σ_{xx} and σ_{yy}, which are responsible for the buckling, as well as the perpendicular stress state σ_{zz}. A high compressive perpendicular stress σ_{zz} supports and stabilizes the structure, so that failure is more unlikely. Buckling failure is defined as a function of the local compressive stress state, the initial yield strength σ_v, the horizontal buckling strength f_{tb} and geometric scaling factors η_x, η_y. The corresponding plastic flow is based on a fully associative approach.

Shearing failure is modelled using an anisotropic Mohr-Coulomb yield surface. The shear failure in transverse direction is defined using a strength anisotropy (joint). The initial shearing strength of the joint is defined as

$$F_{MC,J} = |\tau_{Res}| + \sigma_n \tan\varphi_J - c_J = 0, \tag{2.16}$$

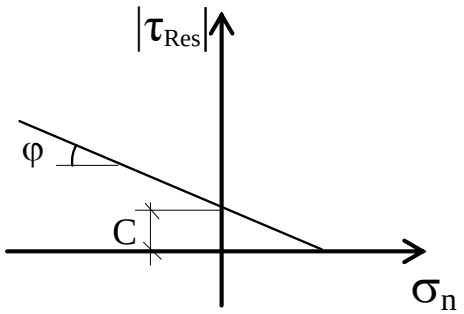

Fig. 2-19: Laminated sheet package – Mohr-Coulomb friction-based yield criterion

where τ_{Res} is the shear stress in joint; σ_n is the normal joint stress perpendicular to the joint ($\sigma_n \equiv \sigma_{zz}$ for the transversal joint), φ_J *is* the initial friction angle and c_J is the initial cohesion. A depiction of this failure criterion is given in Fig. 2-19. It can clearly be seen that compressive stresses strengthen the material, whereas tensile stress states weaken the material shear strength. A non-associated flow rule is applied for the anisotropic Mohr-Coulomb model. Using a dilatancy angle ψ_J for each joint the corresponding plastic potential reads:

$$Q_{MC,J} = |\tau_{Res}| + \sigma_n \tan\psi_J, \tag{2.17}$$

The laminated sheets might fail, if tension is applied in the direction perpendicular to the transverse plane. Therefore, an additional anisotropic tension cut-off yield criterion is defined for each joint as

$$F_{T,J} = \sigma_n - f_{t,J} = 0 \tag{2.18}$$

where $f_{t,J}$ is the initial tensile strength of the respective joint. This tension cut-off yield surface allows a more realistic description of the material strength. An associated flow rule is applied for this yield surface.

Once yielding occurs, it is conservative to assume that the residual strength of the anisotropies are reduced compared to the initial values. Therefore, the initial values are replaced by residual values, e.g. the initial friction angle of the transverse joint φ_J is replaced by φ_J^*.

An illustration of the orientation of the shear strength anisotropies is given in Fig. 2-20. The transverse joint is oriented, so that the local x- and y-axes define the shearing plane. Additional, combinations can be defined for the local joint orientations using the *direc* flag (See TBDATA declaration for more details).

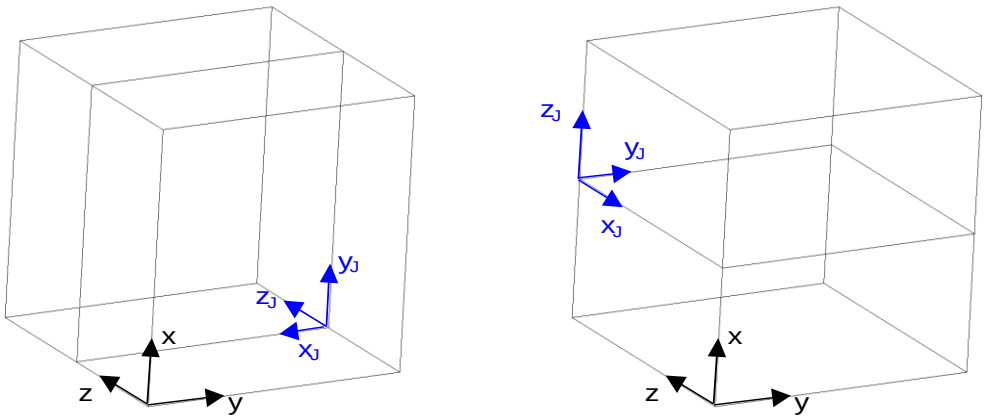

transverse joint $direc = 0$ transverse joint $direc = 1$

Fig. 2-20: Laminated sheet package – joint orientation (blue) with respect to local ESYS coordinate system (black)

2.7.1. Material parameters – standard model (Law 140)

LAW 140 is the standard material model for laminated sheet package with multilinear hardening curve and compressive buckling strength. Failure of laminated sheet package is described using Mohr-Coulomb based in-plane shear strengths. The base material strength is described using a von Mises approach with multi-linear hardening/softening curve. A buckling strength anisotropy can phenomenologically be described using an additional buckling yield surface. The parameters of law 140 are summarized in Table 2.22.

Table 2.22: Laminated sheet package – parameters of the standard model

	1	2	3	4	5	6	7	8	9	10
1-10 base	**140**	σ_v	f_{tb}	η_x	η_y				nkp	
11-20 v.Mises	κ_1	κ_2	κ_3	κ_4	κ_5	κ_6	κ_7	κ_8	κ_9	κ_{10}
21-30 v.Mises	Ω_1	Ω_2	Ω_3	Ω_4	Ω_5	Ω_6	Ω_7	Ω_8	Ω_9	Ω_{10}
31-40 1. joint	φ_{J1}	c_{J1}	ψ_{J1}	φ_{J1}^*	c_{J1}^*	$f_{t,J1}$			$f_{t,J1}^*$	
41-50 2. joint										
51-60										wr
61-70	Elem	Intpt	eps	geps	maxit	cutmax			algo	ktuser
71-80	dvm	dcb	dj1						direc	rsc_flag

General parameters:

parameter	description	SI unit	range
direc	orthogonal direction with respect to sheets 0 – z-direction 1 – x-direction 2– y-direction	[-]	0…2
rsc_flag	joint residual strength coupling flag 0 – coupling is enabled 1 – coupling is enabled 2 – coupling is disabled 3 – coupling is enabled	[-]	0…3
dvm	deactivate von Mises yield surface 0 – activated 1 – deactivated	[-]	0, 1
dcb	deactivate compressive buckling yield surface 0 – activated 1 – deactivated	[-]	0, 1
dj1	deactivate transversal joint 1 0 – activated 1 – deactivated	[-]	0, 1

Virtual sheet package material (homogeneous base material) parameters:

- parameters of the von Mises yield surface:

parameter	description	SI unit	range
σ_v	initial yield strength	[N/m²]	$\sigma_v > 0$
nkp	number of hardening strains/stresses	[-]	0..10
κ_i	plastic strains i	[-]	$\kappa_{i+1} > \kappa_i > 0$
Ω_i	Relative yield stress at point i	[-]	$\Omega_{i+1} > \Omega_i > 1$

- parameters of the compressive buckling strength yield surface:

parameter	description	SI unit	range
f_{tb}	horizontal tensile buckling sheet strength	[N/m²]	$f_{tb} > 0$
η_x	geometric factor scaling the compressive strength in x direction	[N/m²]	$\eta_x > 0$
η_y	geometric factor scaling the compressive strength in y direction	[N/m²]	$\eta_y > 0$

Sheet joint material parameters

The shear joint strength anisotropy is situated according to the direc flag. The orientation follows from the direc flag (0: z-direction, 1: x-direction, 2: y-direction).

- parameters of the anisotropic Mohr-Coulomb yield surface:

parameter	description	SI unit	range
φ_{Ji}	initial friction angle of joint *1*	[°]	$0° \le \varphi_{Ji} < 90°$
c_{Ji}	initial cohesion of joint *1*	[N/m²]	$c_{Ji} \ge 0$
ψ_{Ji}	dilatancy angle of joint *1*	[°]	$0° \le \psi_{Ji} \le \varphi_{Ji}$
φ^*_{Ji}	residual friction angle of joint *1*	[°]	$0° \le \varphi^*_{Ji} \le \varphi_{Ji}$
c^*_{Ji}	residual cohesion of joint *1*	[N/m²]	$0 \le c^*_{Ji} \le c_{Ji}$
$f_{t,J1}$	initial uniaxial tensile strength of joint 1	[N/m²]	$f^*_{tJ1} \le f_{tJ1}$
$f^*_{t,J1}$	residual uniaxial tensile strength of joint 1	[N/m²]	$0 < f^*_{tJ1}$

2.7.2. Material parameters – extended model with stamped packetization (Law 150)

Law 150 extends the standard laminated sheet package model (Law 140) by adding support for stamped packetization.

A stamping of the laminated sheets results in stamped packetization points with increased cohesion. Therefore, the material model includes a stamped packetization option (dj2=0), which adapts the cohesive strength computation.

In this case the apparent cohesion is derived as the Euclidean sum of the user defined effective in-plane shear strengths τ_x and τ_y, so that

$$c_{eff} = \sqrt{\tau_x^2 + \tau_y^2}. \tag{2.19}$$

Once yielding occurs, the strength is reduced based on residual values

$$c_{eff}^* = \sqrt{\tau^{*2}_x + \tau^{*2}_y}. \tag{2.20}$$

The friction angle and dilatancy is fixed to 15° or $\mu = 0.27$ (sheet metal on sheet metal).

Please note that the material model can either be specified with the base joint strength (option dj1 = 0) or the stamped packetization strength (option dj2=0). The two yield surfaces cannot be activated at the same time. The following combinations are valid

- dj1 = 0, dj2 = 1: joint definition of standard model (law 140)
- dj1 = 1, dj2 = 0: joint definition for stamped packetization
- dj1 = 1, dj2 = 1: joint failure is deactivated

The parameters of law 150 are summarized inTable 2.23. The model uses the same layout as law 140. The additional parameters are highlighted in bold.

Table 2.23: Laminated sheet package – parameters of the extended model with optional stamped paketization

	1	2	3	4	5	6	7	8	9	10
1-10 base	**150**	σ_v	f_{tb}	η_x	η_y				nkp	
11-20 v.Mises	κ_1	κ_2	κ_3	κ_4	κ_5	κ_6	κ_7	κ_8	κ_9	κ_{10}
21-30 v.Mises	Ω_1	Ω_2	Ω_3	Ω_4	Ω_5	Ω_6	Ω_7	Ω_8	Ω_9	Ω_{10}
31-40 1. joint	φ_{J1}	c_{J1}	ψ_{J1}	φ^*_{J1}	c^*_{J1}	$f_{t,J1}$			$f^*_{t,J1}$	
41-50 2. joint	$\boldsymbol{\tau_{x,J2}}$	$\boldsymbol{\tau^*_{xJ,2}}$	$\boldsymbol{\tau_{y,J2}}$	$\boldsymbol{\tau^*_{y,J2}}$	$\boldsymbol{f_{t,J2}}$	$\boldsymbol{f^*_{t,J2}}$				
51-60										wr
61-70	Elem	Intpt	eps	geps	maxit	cutmax			algo	ktuser
71-80	dvm	dcb	dj1	**dj2**					direc	rsc_flag

General parameters:

parameter	description	SI unit	range
dj1	deactivate transversal joint 1 deactivated if dj1 > 0	[-]	0, 1 $dj1 > 0, if\ dj2 = 0$
dj2	deactivate stamped packetization shear strength joint 2 deactivated if dj2 > 0	[-]	0, 1 $dj2 > 0, if\ dj1 = 0$

Stamped packaging shear failure parameters

This joint set is situated in the same plane as the sheet joint 1. Its friction angle and dilatancy is fixed to 15° or $\mu = 0.27$ (sheet metal on sheet metal). The orientation

follows from the direc flag (0: z-direction, 1: x-direction, 2: y-direction). The effective cohesion is the Euclidean sum of the respective shear strengths.

- parameters of the anisotropic Mohr-Coulomb yield surface:

parameter	description	SI unit	range
$\tau_{x,J2}$	initial shear strength of joint 2 in local x direction	[N/m^2]	$\tau^*_{xJ2} \leq \tau_{xJ2}$
$\tau^*_{x,J2}$	residual shear strength of joint 2 in local x direction	[N/m^2]	$0 \leq \tau^*_{xJ2}$
$\tau_{y,J2}$	initial shear strength of joint 2 in local y direction	[N/m^2]	$\tau^*_{yJ2} \leq \tau_{yJ2}$
$\tau^*_{y,J2}$	residual shear strength of joint 2 in local y direction	[N/m^2]	$0 \leq \tau^*_{yJ2}$
$f_{t,J2}$	initial uniaxial tensile strength of joint 2	[N/m^2]	$f^*_{t,J2} \leq f_{t,J2}$
$f^*_{t,J2}$	residual uniaxial tensile strength of joint 2	[N/m^2]	$0 \leq f^*_{t,J2}$

2.7.3. State variables

In this model **7** state variables are defined. The state variables are summarized in Table 2.24.

Table 2.24: Laminated sheet package - state variables

state variable	description
1	number representing the activity of individual yield surfaces (failure modes)
2	accumulated plastic multiplier of von Mises yield surface
3	accumulated plastic multiplier of the compressive buckling strength yield surface in x -direction
4	accumulated plastic multiplier of the compressive buckling strength yield surface in y -direction
5	accumulated tangential plastic strains due to Mohr-Coulomb failure of the joint
6	accumulated normal plastic strains due to Mohr-Coulomb failure of the joint
7	accumulated normal plastic strains due to tensile failure of the joint

2.7.4. Activity encoding

The activity of the individual yield surfaces is encoded into a single number. The following table shows the encoding if a single yield surface fails. If multiple yield surfaces fail then the corresponding numbers are added, e.g. 1 001 represents shear failure of joint set 1 and failure of the von Mises yield surface.

number	activity
1	von Mises
10	Buckling x
100	Buckling y
1 000	shear failure of joint set
10 000	tensile failure of joint set

2.8. Implicit creep

The multiPlas library incorporated an implicit creep option. In this context the elastic strain is redefined as

$$\boldsymbol{\varepsilon^{el}} = \boldsymbol{\varepsilon^{tot}} - \boldsymbol{\varepsilon^{pl}} - \boldsymbol{\varepsilon^{cr}}, \tag{2.21}$$

where $\boldsymbol{\varepsilon^{cr}}$ is the creep strain vector. The evolution of the creep strain is defined in terms of an equivalent creep strain rate $\dot{\varepsilon}_v^{cr}$

$$\dot{\boldsymbol{\varepsilon}}^{\boldsymbol{cr}} = \frac{3}{2}\frac{\dot{\varepsilon}_v^{cr}}{\sigma_v}\boldsymbol{s}, \tag{2.22}$$

where $\boldsymbol{s}$ is the deviatoric stress and σ_v is the von Mises stress, given by

$$\sigma_v = \sqrt{3J_2} = \sqrt{\frac{3}{2}s_{ij}s_{ij}}. \tag{2.23}$$

The evolution of the equivalent creep strain can be defined by one of the functions defined in the following sub-sections. Up to 18 creep material parameters might be defined.

For each specific creep law, the reference temperature T is the absolute temperature. It is defined using the temperature at the current time step, offset by T_{offset}, so that

$$T = T_{ANSYS} + T_{offset}.$$

For example: The absolute temperature could be calculated by using an offset of 273 K, so that the temperatures in Ansys are still calculated in °C, but are strictly positive during creep law evaluation.

2.8.1. Material parameters

Any basic multiPlas material law can be adapted to incorporate implicit creep. In general, the TBDATA table of the corresponding material is enhanced to a size of 100. Parameters 81-100 are then used for creep specification. The creep law can be chosen with entry 81 (claw). Up-to 18 creep law specific material ocnstants can be provided using entries 82-109. The creep law temperature offset is defined using entry 110 (T_{offset}).

Table 2.25: Creep parameters as addition to general multiplas data table

	1	2	3	4	5	6	7	8	9	10
1-10	LAW									
11-20										
21-30										
31-40										
41-50										
51-60										wr
61-70	Elem	Intpt	eps	geps	maxit	cutmax			algo	ktuser
71-80										
81-90 creep	claw	c_1	c_2	c_3	c_4	c_5	c_6	c_7	c_8	c_9
91-100 creep	c_{10}	c_{11}	c_{12}	c_{13}	c_{14}	c_{15}	c_{16}	c_{17}	c_{18}	T_{offset}

2.8.2. State variables

The creep state variables are added to the state variables of the specific material law. Seven creep state variables are written to the result database if implicit creep is selected. For example, law 17 uses three state variables: the activity number, the plastic state of first yield surface and the plastic state of second yield surface. Therefore, for law 17 the creep strain in x direction is written to SVAR4 and the accumulated creep strain is written to SVAR10, so that in total 3+7=10 state variables are written to the result database.

Table 2.26: Additional creep state variables

state variable local offset	description
1	Creep strain in x direction
2	Creep strain in y direction
3	Creep strain in z direction
4	Creep strain in xy direction
5	Creep strain in yz direction
6	Creep strain in xz direction
7	Accumulated creep strain $\int_0^t \dot{\varepsilon_{cr}} dt$

2.8.3. Norton creep

- claw 10 : Norton law (secondary creep):

$$\dot{\varepsilon}_v^{cr} = c_1 \sigma_v^{c_2} \exp\left(-\frac{c_3}{T}\right), \tag{2.24}$$

Please note that the creep law is evaluated in logarithmic form. Therefore, parameter c_1 has to be input as logarithmic value, e.g. $c_1 = 5$ would be input as LOG(5) in the TBDATA data table entry. In contrast, c_2 and c_3 must be input as regular values.

2.9. Numerical control variables

In this section additional parameters controlling the behavior of multiPlas are presented. In TBDATA-tables in previous sections these parameters are marked by a grey background. The TBDATA-definition of the numerical control variables are shown in Table 2.27. In most cases the recommended values can be applied.

Table 2.27: Parameters of multiPlas numerical control variables

	1	2	3	4	5	6	7	8	9	10
1-10										
11-20										
21-30										
31-40										
41-50										
51-60										wr
61-70	Elem	Intpt	eps	geps	maxit	cutmax			algo	ktuser
71-80										

2.9.1. Return mapping related parameters

The first set of parameters, summarized in Table 2.28, control the return mapping algorithm.

Table 2.28: multiPlas return mapping control parameters

parameter	description	recommendation
eps	relative convergence criteria in the return mapping algorithm	10^{-3} (should not be too small)
geps	tolerance for singular systems of equations in multi-surface plasticity return mapping algorithm	10^{-20}
maxit	maximum number of iteration steps in the return mapping algorithm	100
cutmax	maximum number of local bisections in the return mapping algorithm	10
algo	return mapping algorithm 0 – automatic selection 1 – cutting plane algorithm 2 – closest point return mapping	0 – automatic selection
ktuser	elasto-plastic tangent flag 0 – elasto-plastic tangent is disabled (linear elastic material matrix is returned) 1 – elasto-plastic tangent is enabled 2 – elasto-plastic tangent is only enabled in perturbation analysis (works only with custom executable)	0 – elasto-plastic tangent is disabled

2.9.2. Output related parameters

For debugging purposes multiPlas allows the output of additional information during the return mapping for a single integration point. Table 2.29 summarizes the parameters controlling the output messages.

Table 2.29: multiPlas output control parameters.

parameter	description
wr	verbosity level of outputs (0 - output is disabled)
Elem	element number
Intp	integration point number in element Elem

If during the simulation the return mapping algorithm fails, then multiPlas forces a global bi-section of the load increment. In that case Ansys issues the following message:

**** NOTE *** CP = 24.423 TIME= 10:30:27*
One or more elements have become highly distorted. Excessive distortion of elements is usually a symptom indicating the need for corrective action elsewhere. Try incrementing the load more slowly (increase the number of substeps or decrease the time step size). You may need to improve your mesh to obtain elements with better aspect ratios. Also consider the behavior of materials, contact pairs, and/or constraint equations. If this message appears in the first iteration of first substep, be sure to perform element shape checking.

By setting the verbosity level wr to a value larger than zero, the following additional message is printed by multiPlas:

multiPlas stress calculation failed for element: 104 integration point: 2 global bisection is performed

This message helps to identify the critical element. Furthermore, the file *multiPlas_stress_calculation_failed_104_2.txt* is written. In this file the input parameters and the state variables are stored for the critical point.

3. Best practice

3.1. Material parameters

All material parameters must be defined in a consistent unit system, e.g. N, kg, m, s. Furthermore, the material parameters must be defined in the same unit system as the other model parameters, e.g. geometry parameters. Especially in Ansys Workbench it is recommended to double-check that the unit system chosen in Workbench is identical to the unit system of the multiPlas material parameters.

In general, the multiPlas material parameters have a clear physical meaning. As a result, the user can check if the parameters are in a reasonable range for the particular material, e.g. by comparing the parameters with typical values in the literature. Some of the parameters might be correlated, e.g. the fracture energy, the tensile strength and the Young's modulus. Consequently, if one of those parameters is modified, the user should check if the relationship to the other parameters is still valid, e.g. the volume specific fracture energy must be considerably larger than the elastic energy stored in the element. A simple test if the parameters are consistent is to run single element tests, as demonstrated in the multiPlas training. In this context, one important point is that these tests should be run with an element with comparable size as in the final application and with the same multiPlas material macros. If these tests already fail, the material properties are in most cases not in balance and should be adjusted accordingly.

Another important point is that for numerical stability no material parameter should be set exactly equal to zero. There are two exceptions: In the isotropic three-dimensional Mohr-Coulomb model (law 1) the friction angle can be set to zero which results in the Tresca criterion and in the geological Drucker-Prager model (law 40) the parameter beta (slope of the cone) can be set to zero which yields the von Mises criterion. Even the residual strength parameters should not be set equal to zero. In most applications residual strength values of 1% of the corresponding initial strength values are close enough to zero.

In some of the multiPlas material models a non-associated flow rule is applied and the direction of plastic strains is defined in terms of a dilatancy angle, e.g. models with Mohr-Coulomb yield surfaces, or dilatancy factors, e.g. models which are based on Drucker-Prager yield surfaces. A dilatancy value close to zero implies in a physical sense ideally smooth friction surface. This might lead to extreme convergence difficulties. For example, in the case of shear failure the corresponding normal stress component cannot be redistributed if the dilatancy value is zero. In multiPlas dilatancy angles larger than 5° and dilatancy factors larger than 0.1 are recommended. Please note, that smaller values might work as well, but generally result in poor convergence behavior.

The material parameters are automatically checked by multiPlas. If a parameter is not valid, the simulation is stopped, and an error message is issued. Please note, that multiPlas is called the first time when the solution starts with the calculation of the element matrices and vectors. If the simulation fails with a fatal error in this stage (Ansys is closed at the beginning of the solution phase), then please check the error file or the log file for multiPlas error messages.

3.2. Modelling and meshing

The convergence in a nonlinear analysis with multiPlas is not only influenced by the material parameters but also by the model itself, e.g. the finite element mesh. In general, there are no restrictions on the type of mesh, e.g. structured or unstructured. Because the material law is only evaluated at discrete points, the so-called integration points, the distribution of these points significantly influence the convergence behavior. The position of the integration points depends on the element type, the element size, and the element shape. In a nonlinear analysis with multiPlas the integration points should be uniformly distributed. Consequently, the element size should not significantly vary in those parts of the structure where plasticity is expected. Furthermore, distorted elements or elements with bad aspect ratio should be avoided. In this context in large deformation analysis the mesh quality can be improved during the simulation using the Ansys rezoning feature, cf. Ansys user manual.

Another aspect in this context is the element size. Every integration point represents a certain domain in the structure. It is assumed that the material behavior in this domain can be represented by the material behavior at the integration point. Consequently, if the material fails at the integration point, the material fails in the domain associated to the integration point. In a coarse mesh this might result in a sudden release of energy which can cause convergence issues. To avoid these issues, the finite element mesh should be sufficiently fine.

The nonlinear analysis of a structure is generally time-consuming. Therefore, the model should be simplified as much as possible. For example, if plane stress or plane strain conditions apply, then the analysis should be performed with a 2D mesh. In a full 3D model with plane stress conditions the out-of plane stresses might not be exactly zero. Furthermore, the stresses might not be constant over thickness due to numerical inaccuracies. If more than one element is used over thickness, then the non-constant stresses over thickness might result in divergence because of bifurcation problems, especially if softening is applied. All these problems can be avoided by using a 2D model.

Furthermore, any symmetry in the model should be used. For example, the uniaxial compression test of a cylinder should be analyzed with an axisymmetric 2D model. As a result, the numerical effort is significantly reduced, and the convergence behavior generally improves. To verify the symmetry conditions, it is recommended to perform a linear elastic analysis and compare the results to a simulation with the full model, before running a nonlinear analysis with the reduced symmetric model.

3.3. Nonlinear structural analysis and convergence

In simulations with multiPlas a generally nonlinear system of equations is solved in an iterative way using the Newton-Raphson algorithm. In this context the convergence of this algorithm can be influenced by several options. It is assumed that all commands in this section are issued in the solution phase (**/SOLU**) before the **SOLVE** command is called. Please review the Ansys manual for a detailed description of the individual commands.

The Newton-Raphson algorithm requires a division of the load-step into sub-steps. In Ansys APDL the sub-steps can be defined by the **NSUBST** or the **DELTIM** command. Note that both commands are equivalent. The definition of sub-steps includes an initial step size, a maximum step size and a minimum steps size. It is recommended that the initial step size is chosen such that the material behavior remains linear elastic (no plasticity). This allows the user to check if the model is stable for linear elastic behavior. To allow an automatic selection of the actual step size, the minimum and maximum step size should not be identical to the initial step size. Furthermore, the automatic time stepping should be switched on: **AUTOTS**, ON.

In general, the standard Ansys settings for a non-linear analysis can be used with multiPlas. The default settings are set by the APDL-command: **SOLCONTROL**, ON. A complete listing of the defaults set by **SOLCONTROL**, ON can be found in the Ansys manual.

In most multiPlas simulations the default maximum number of equilibrium iteration steps within one sub-step is too low. Therefore, it is recommended to increase the number of maximum equilibrium iteration steps. For example, **NEQIT**,60 sets the maximum number of iteration steps to 60. The actual maximum number of equilibrium iteration steps depends on the application. But a value between 60 and 200 is recommended for multiPlas.

Ansys tries to improve the convergence by using a predictor for the first sub step. In simulations with multiPlas it is recommended to switch off this feature. This can be done with the APDL command: **PRED**, OFF, , OFF.

Ansys automatically performs a global bisection if the maximum equivalent plastic strain within one sub step becomes larger than 15%. In simulations with large plastic strains this limit might be too tight. As a result, global bisections (reduction of the step size) might be performed for many steps, even when the simulation converged for a sub-step. This limit can be relaxed by the **CUTCONTROL** command. For example, **CUTCONTROL**, PLSLIMIT, 0.5 increases the limit to 50%.

Additionally, the convergence criterion can be modified with the **CNVTOL** command. The default values should be modified very carefully. If the convergence criterion is too loose the simulation might converge just in a few iteration steps, but the error in the Newton-Raphson iteration, e.g. the out-of-balance forces, might become large. As a result, the structure might not be in equilibrium. In the opposite case, if the convergence criterion is too strict then a lot of iteration steps might be necessary for convergence, or the simulation might not converge at all until the maximum number of equilibrium iteration steps is reached. The advantage of a strict convergence criterion is, if the iteration converges, that the error in the Newton-Raphson iteration becomes generally small and the equilibrium point is well defined. Consequently, the definition of convergence criteria is always a compromise between accuracy and simulation time.

3.3.1. Elasto-plastic tangent

multiPlas supports an elasto-plastic tangent. The elasto-plastic tangent is calculated by multiPlas if the control parameter ktuser is set equal to 1. Otherwise, the linear elastic material matrix is returned by multiPlas. In general, the elasto-plastic tangent should improve the convergence behavior. But this is not always the case because of several reasons. The material models in multiPlas support hardening/softening and non-associated flow. As a result, the tangent becomes generally unsymmetric. Furthermore, the tangent might not be positive definite, e.g. the tangent might have zero eigenvalues in the case of perfect plasticity or negative eigenvalues in the case of softening. On element level this is not a big problem. But if the global stiffness matrix, which is assembled from the element tangents, has zero or negative eigenvalues, the system becomes unstable, and the Newton-Raphson iteration procedure diverges. Another problem is that a consistent (algorithmic) tangent is only available for the closest point return mapping procedure of multiPlas. If the cutting plane return mapping is applied, then the return mapping algorithm cannot be consistently linearized, and the continuum tangent is calculated which generally deviates from the consistent tangent. Finally, in the case of changing activities within the framework of multi-surface plasticity, the tangent is not defined at all.

Because of all these reasons it is not recommended to use the elasto-plastic tangent in complex simulations (recommendation: ktuser=0). As a result, the global solution procedure becomes a modified Newton-Raphson algorithm, which shows a slower convergence. But the solution of the global system of equations is more stable. In simulations without any other nonlinearity besides multiPlas, the initial stiffness Newton-Raphson solution procedure, which is switched on by **NROPT**, INIT, can be used. The advantage of this procedure is that in the case of a sparse solver the global stiffness matrix is only factorized once in the beginning of the simulation. As a result, the numerical effort for solving the global system of equations reduces significantly for every iteration step. In the case of additional nonlinearities, e.g. contact, geometrical nonlinearity or Ansys nonlinear material models, the standard Newton-Raphson algorithm can be applied, e.g. **NROPT**, AUTO.

However, if the computation of the elasto-plastic tangent is enabled in multiPlas then the full Newton-Raphson iteration with unsymmetric matrices must be applied. The Ansys Newton-Raphson procedure can be switched to unsymmetric by the APDL command **NROPT**, UNSYM. Please note that this command might also influence the tangent which is calculated for Ansys contact elements if friction is enabled.

3.4. How to solve convergence problems

The convergence behavior in a nonlinear simulation is influenced by many parameters, e.g. loads, boundary conditions, mesh, modelling or material parameters. If a simulation does not converge then a deep understanding of the model itself and of the solution procedure is required to identify the reason for the convergence problems and to overcome these problems. This section is a collection of hints and tips which should help to solve convergence problems.

1. Run the simulation in batch mode and check the Ansys output file (*.out) and the Ansys error file (*.err) for error messages and warnings. Try to fix these issues and rerun the simulation.
2. The Netwon-Raphson algorithm is an iterative procedure for the solution of a nonlinear system of equations. The algorithm converges if the initial guess is not too far away from the final solution. Consequently, the sub-step definition (**DELTIM** or **NSUBST**) should allow a considerable reduction of the step size.
3. Depending on the loading conditions and the applied solution procedure, convergence might become impossible during the simulation. Consequently, the divergence of the solution might not be a problem at all.
    - In a load controlled simulation, the load factor within a load step must be strictly increasing. As a result, the solution fails to converge if the load bearing capacity is reached. In that case the tangent becomes horizontal in the global load-displacement curve. Consequently, a global softening behavior of the structure cannot be simulated with load control. It is to be noted that softening on element level does not necessarily result in global softening.
    - Global softening can be simulated with a direct displacement control. In this context the loads are replaced by equivalent displacement boundary conditions. In a displacement-controlled simulation the displacement factor must be strictly increasing within a load step. Consequently, direct displacement control cannot handle snap-back and snap-through phenomena. In that case the tangent in the global load-dis placement curve becomes vertical.
    - Snap-back and snap-through phenomena can be modeled with the arc length method, cf. Ansys APDL command **ARCLEN**, which is a combination of load and displacement control. The arc length method can be also applied in cases where loads cannot be replaced by equivalent displacement boundary conditions.
4. The convergence behavior itself should be analyzed.
    - If the solution converges, e.g. the out-of-balance loads reduce, but the convergence criterion is not satisfied before a global bisection is performed then the number of equilibrium iterations should be increased, cf. Ansys APDL command **NEQIT**. Additionally, the convergence criteria could be relaxed, cf. Ansys APDL command **CNVTOL**.
    - An oscillation in the convergence behavior is an indicator for bifurcation problems. Consequently, the solution is no longer unique. This might happen if a symmetric problem is analyzed with a full model. In that case the model should be reduced by considering any symmetry. Another approach is to force one of the solution paths. One option is to introduce imperfections in the system. This might be difficult for complex systems. Another option is to relax for this step the convergence criterion slightly above the lower oscillation value. In the following steps the convergence criterion should be set back.

- A global bisection might be caused by multiPlas. If the return mapping procedure on material point level fails, then a global bisection is performed. This case can be identified by the following message: "multiPlas stress calculation failed for element: <element_id> integration point: <int_point_id> global bisection is performed" in the Ansys output file. This output is only written if the multiPlas parameter wr is larger than zero. In that case the multiPlas material parameters as well as the numerical control parameters should be checked.

5. Reduce the complexity of the model. If the simplified model does not converge then in most cases the complex model will also not converge. If the simplified model converges then increase step by step the complexity. This approach helps to identify the source of the convergence problems.
   - Run a simulation without the nonlinear models of multiPlas. This can be realized by setting multiPlas material to law=0 or by deleting the corresponding Ansys user tables, cf. Ansys APDL command **TBDELE**.
   - If possible, disable other nonlinearities in the model, e.g. geometrical nonlinearity, cf. Ansys APDL command **NLGEOM**, or contact.
   - Run single element tests for the multiPlas material parameters and the typical element size of the critical region.
   - Use an associated flow rule and ideal plastic behavior
   - In the case of softening behavior, reduce the brittleness of the material, e.g. increase the fracture energy.
   - In material models with joints, try to reduce the number of yield surfaces in the model. Run a simulation without joints. Run a simulation without intact failure. In the case of multiple joints run simulations for every joint set separately.
   - If the closest point return mapping procedure is applied in multiPlas then switch to the cutting plane return mapping by setting the multiPlas numerical control variable algo=1.
   - Disable the elasto-plastic tangent by setting the multiPlas numerical control parameter ktuser=0. And change the Newton-Raphson procedure from unsymmetric to auto selection or initial, cf. Ansys APDL command **NROPT**.
   - Reduce the initial sub-step size, cf. Ansys APDL commands **DELTIM** or **NSUBST**, such that the multiPlas material models remain in the elastic domain in the initial step.

3.5. Post-processing

Generally, Ansys extrapolates element results from the integration points to the nodes if the element is elastic. If the element becomes plastic the results are copied from the integration points to the nodes. Because the element results are averaged at the nodes, the interpretation of the results might become difficult if one element is connected to an elastic element as well as a plastic element. Therefore, it is recommended to disable the extrapolation of the element results for all elements by applying the Ansys APDL command **ERESX**, NO in the solution phase before the SOLVE command is called.

3.5.1. Equivalent plastic strain

The equivalent plastic strain is a scalar measure of the plastic strain tensor. It shows the quantitative activity and can be used to identify the areas in which local load shifting or material failure / crack formation take place. In multiPlas the von Mises equivalent plastic strain definition is applied. In the incremental form the equivalent plastic strain increment can be written as

$$\begin{aligned}\Delta\varepsilon_{pl,eqv} &= \sqrt{\frac{2}{3}\Delta\varepsilon_{pl}:\Delta\varepsilon_{pl}} \\ &= \sqrt{\frac{2}{3}\left[\Delta\varepsilon_{pl,xx}^2+\Delta\varepsilon_{pl,yy}^2+\Delta\varepsilon_{pl,zz}^2+\frac{1}{2}(\Delta\varepsilon_{pl,xy}^2+\Delta\varepsilon_{pl,yz}^2+\Delta\varepsilon_{pl,xz}^2)\right]}\end{aligned} \tag{3.1}$$

Consequently, the equivalent plastic strain is an additional history variable which is updated after every load increment.

In the post-processing (/POST7) the activities can be plotted with one of the following commands:

PLESOL, EPPL, EQV

PLNSOL, EPPL, EQV

3.5.2. Plastic activity

The plastic activity shows which yield surfaces are active in the current equilibrium state. A yield surface is marked active if this yield surface has a positive plastic multiplier. Consequently, the yield surface was violated during the return-mapping procedure and the stress state at the end of the return-mapping process is on this yield surface. This allows the identification of failure mechanisms and the cause of load shifting. The plastic activity is path dependent. A yield surface can be activated and deactivated more than once during a load case.

The plastic activity value is stored in the first state variable of nonlinear multiPlas material models. The meaning of the activity value depends on the individual material models. The encoding of the activity value is shown in the subsections of sections 2 and **Error! Reference source not found.**.

To plot the activity value, the state variables must be stored in the result file. Please execute the following command in the solution phase before solving the global system of equations (**SOLVE**):

OUTRES, SVAR, <Freq> (<Freq> can be replaced by an integer, LAST or ALL. Please refer to the Ansys APDL manual for a comprehensive description of the OUTRES command)

In the post-processing **(/POST1**) the activities can be plotted with one of the following commands:

PLESOL,SVAR,1

PLNSOL,SVAR,1

4. References

[1]	Bathe, K. J.: Finite element procedures. Prentice Hall, 1985
[2]	Bažant, Z.P.; Oh, B.H.: Crack band theory for fracture of concrete. Materials and Structures, RILEM, 93 (16), S. 155-17
[3]	Berndt, E.: Zur Druck- und Schubfestigkeit von Mauerwerk – experimentell nachgewiesen an Strukturen aus Elbsandstein. Bautechnik 73, S. 222-234 Ernst & Sohn, Berlin (1996)
[4]	Ganz, H.R.: Mauerwerkscheiben unter Normalkraft und Schub. ETH Zürich, Institut für Baustatik und Konstruktion. Dissertation. Birkhäuser Verlag Basel (1985)
[5]	Grosse, M.: Zur numerischen Simulation des physikalisch nichtlinearen Kurzzeittragverhaltens von Nadelholz am Example von Holz-Beton-Verbundkonstruktionen. Dissertation, Bauhaus-Universität Weimar (2005)
[6]	Mann, W.; Müller, H.: Schubtragfähigkeit von gemauerten Wänden und Voraussetzungen für das Entfallen des Windnachweises. Berlin: Ernst u. Sohn. In: Mauerwerk-Kalender (1985)
[7]	Pluijm, R. van der: Shear behaviour of bed joints. Proc. 6th North American Masonry Conference, S. 125-136 (1993)
[8]	Pölling, R.: Eine praxisnahe, schädigungsorientierte Materialbeschreibung von Stahlbeton für Strukturanalysen. Ruhr-Universität Bochum, Dissertation (2000)
[9]	Schlegel, R.: Numerische Berechnung von Mauerwerkstrukturen in homogenen und diskreten Modellierungsstrategien. Dissertation, Bauhaus-Universität Weimar, Universitätsverlag (2004), ISBN 3-86068-243-1
[10]	Simo, J. C.; Hughes, T. J. R.: Computational Inelasticity. Springer, 1998
[11]	Simo, J.C.; Kennedy, J.G.; Govindjee, S.: Non-smooth multisurface plasticity and viscoplasticity. Loading / unloading conditions and numerical algorithms. Int. Journal for numerical methods in engineering. Vol. 26, 2161-2185 (1988)
[12]	Will, J.: Beitrag zur Standsicherheitsberechnung im geklüfteten Fels in der Kontinuums- und Diskontinuumsmechanik unter Verwendung impliziter und expliziter Berechnungsstrategien: Bauhaus Universität Weimar, Dissertation 1999, Berichte Institut für Strukturmechanik 2/99